ARTICLE

doi:10.1038/nature17998

NMDAR inhibition–independent antidepressant actions of ketamine metabolites

Panos Zanos[1], Ruin Moaddel[2], Patrick J. Morris[3], Polymnia Georgiou[1], Jonathan Fischell[4], Greg I. Elmer[1,5,6], Manickavasagom Alkondon[7], Peixiong Yuan[8], Heather J. Pribut[1], Nagendra S. Singh[2], Katina S. S. Dossou[2], Yuhong Fang[3], Xi-Ping Huang[9], Cheryl L. Mayo[6], Irving W. Wainer[2]†, Edson X. Albuquerque[5,7,10], Scott M. Thompson[1,4], Craig J. Thomas[3], Carlos A. Zarate Jr[8] & Todd D. Gould[1,5,11]

Major depressive disorder affects around 16 per cent of the world population at some point in their lives. Despite the availability of numerous monoaminergic-based antidepressants, most patients require several weeks, if not months, to respond to these treatments, and many patients never attain sustained remission of their symptoms. The non-competitive, glutamatergic NMDAR (*N*-methyl-D-aspartate receptor) antagonist (*R*,*S*)-ketamine exerts rapid and sustained antidepressant effects after a single dose in patients with depression, but its use is associated with undesirable side effects. Here we show that the metabolism of (*R*,*S*)-ketamine to (2*S*,6*S*;2*R*,6*R*)-hydroxynorketamine (HNK) is essential for its antidepressant effects, and that the (2*R*,6*R*)-HNK enantiomer exerts behavioural, electroencephalographic, electrophysiological and cellular antidepressant-related actions in mice. These antidepressant actions are independent of NMDAR inhibition but involve early and sustained activation of AMPARs (α-amino-3-hydroxy-5-methyl-4-isoxazole propionic acid receptors). We also establish that (2*R*,6*R*)-HNK lacks ketamine-related side effects. Our data implicate a novel mechanism underlying the antidepressant properties of (*R*,*S*)-ketamine and have relevance for the development of next-generation, rapid-acting antidepressants.

Major depressive disorder is common, affecting about 16% of the world population at some point in their lives, and is associated with serious health and socioeconomic consequences[1,2]. Current pharmacotherapies, including monoaminergic-acting antidepressants, require prolonged administration (weeks if not months) for clinical improvement. This lag time, as well as a high non-response rate, emphasizes the need for better antidepressant medications[3]. The non-competitive, glutamatergic NMDAR antagonist (*R*,*S*)-ketamine (ketamine) has demonstrated rapid and robust efficacy as an antidepressant by improving core depressive symptoms including depressed mood, anhedonia, and suicidal thoughts in treatment-refractory unipolar and bipolar depressed patients when administered at sub-anaesthetic doses[4–8]. Remarkably, these actions are observed within hours after a single administration, and persist on average for 1 week. While discovery of the clinical antidepressant efficacy of ketamine for the treatment of depression has elicited tremendous excitement in the field, its potential for widespread clinical use is limited owing to its abuse liability and capacity to produce dissociative effects even when administered at low doses[9]. There are also unanswered questions about how ketamine works as an antidepressant, which is typically assumed to depend on direct NMDAR inhibition. However, the results of human treatment trials indicate that alternative NMDAR antagonists lack the robust, rapid and/or sustained antidepressant properties of ketamine[10].

Role of NMDAR inhibition in ketamine action

We compared the antidepressant-like effects of ketamine and the classical tricyclic antidepressant desipramine in the mouse forced-swim test (FST) at 1 h (acute) and 24 h (sustained) after administration (Fig. 1a). A 10 mg kg^{-1} dose of ketamine resulted in acute and long-lasting dose-dependent antidepressant effects in the FST, whereas desipramine decreased immobility time only 1 h after injection. To date, most studies assessing the antidepressant effects of ketamine are based on a commonly accepted view that ketamine and its *N*-demethylated metabolite (*R*,*S*)-norketamine are the active agents, the clinical effects of which are due to inhibition of the NMDAR. Additional metabolites (Extended Data Figs 1 and 2a, b) are considered clinically inactive since they do not induce anaesthesia[11]. To determine whether NMDAR inhibition is the main mechanism underlying the antidepressant effects of ketamine, we assessed the effects of the (*S*)- and (*R*)-ketamine enantiomers in the FST (Fig. 1b), novelty-suppressed feeding (NSF) test (Fig. 1c) and learned helplessness test (Fig. 1d). While the NMDAR hypothesis of ketamine action would predict greater efficacy of (*S*)-ketamine since it is a ~3–4-fold more potent inhibitor of the NMDAR than (*R*)-ketamine[12,13], our results, in accordance with a recent report[14], demonstrate a greater potency of (*R*)-ketamine in all three antidepressant-predictive tasks. Notably, this antidepressant effect does not result from higher brain levels of (*R*)-ketamine than of (*S*)-ketamine (Extended Data Fig. 2c–e). Moreover, in contrast to ketamine, we

[1]Department of Psychiatry, University of Maryland School of Medicine, Baltimore, Maryland 21201, USA. [2]Biomedical Research Center, National Institute on Aging, National Institutes of Health, Baltimore, Maryland 21224, USA. [3]Division of Preclinical Innovation, National Center for Advancing Translational Sciences, National Institutes of Health, Rockville, Maryland 20850, USA. [4]Department of Physiology, University of Maryland School of Medicine, Baltimore, Maryland 21201, USA. [5]Department of Pharmacology, University of Maryland School of Medicine, Baltimore, Maryland 21201, USA. [6]Maryland Psychiatric Research Center, University of Maryland School of Medicine, Baltimore, Maryland 21228, USA. [7]Department of Epidemiology and Public Health, Division of Translational Toxicology, University of Maryland School of Medicine, Baltimore, Maryland 21201, USA. [8]Experimental Therapeutics and Pathophysiology Branch, Intramural Research Program, National Institute of Mental Health, National Institutes of Health, Bethesda, Maryland 20892, USA. [9]NIMH Psychoactive Drug Screening Program, Department of Pharmacology and Division of Chemical Biology and Medicinal Chemistry, University of North Carolina Chapel Hill Medical School, Chapel Hill, North Carolina 27516, USA. [10]Department of Medicine, University of Maryland School of Medicine, Baltimore, Maryland 21201, USA. [11]Department of Anatomy and Neurobiology, University of Maryland School of Medicine, Baltimore, Maryland 21201, USA. †Present address: Mitchell Woods Pharmaceuticals, Shelton, Connecticut 06484, USA.

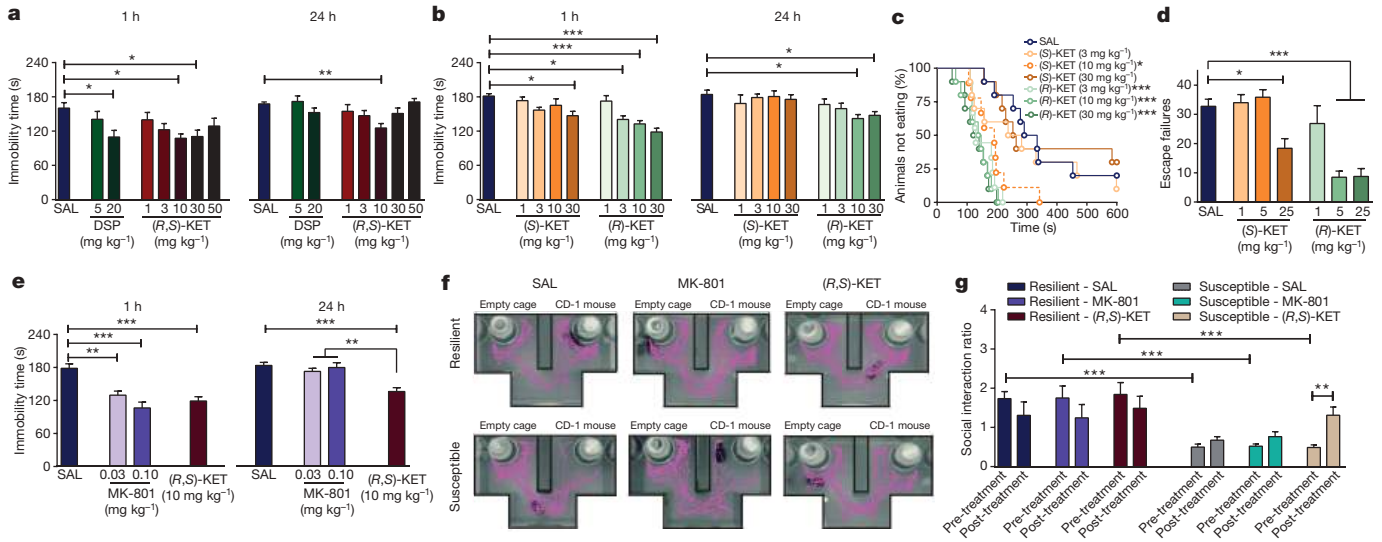

Figure 1 | NMDAR inhibition is not sufficient for the antidepressant actions of ketamine. a, Antidepressant-like responses of (*R*,*S*)-ketamine (KET) and desipramine (DSP) in the forced-swim test (FST) 1- and 24-h after treatment. SAL, saline. **b**–**d**, Compared to (*S*)-KET, (*R*)-KET showed greater and longer-lasting antidepressant-like effects in the FST (**b**), novelty-suppressed feeding (NSF) test (**c**) and learned helplessness test (**d**). **e**–**g**, The alternative NMDAR antagonist MK-801 did not elicit 24-h antidepressant actions in the FST (**e**), and did not reverse social avoidance induced by chronic social defeat stress (**f**, **g**), where purple lines represent the video-tracked movements of mice (**f**). Data are mean ± s.e.m. $*P < 0.05$, $**P < 0.01$, $***P < 0.001$ (see Supplementary Table 1 for statistical analyses and *n* numbers).

demonstrated that the NMDAR antagonist MK-801, which binds at the same receptor site as ketamine, does not exert sustained (24 h) antidepressant-like effects in the FST (Fig. 1e; see also refs 15, 16), or reverse social interaction deficits induced by chronic social defeat stress (Fig. 1g and Extended Data Fig. 3). These findings indicate a probable NMDAR inhibition-independent mechanism underlying the antidepressant responses of ketamine.

Antidepressant actions of ketamine metabolites

Ketamine is stereoselectively metabolised into a broad array of metabolites, including norketamine, hydroxyketamines, dehydronorketamine and the HNKs[17,18] (Fig. 2a and Extended Data Fig. 1). After ketamine administration, (2*S*,6*S*;2*R*,6*R*)-HNK is the major HNK metabolite found in the plasma and brain of mice (Extended Data Fig. 2a, b), and plasma of humans[19]. Similar to previous evidence revealing enhanced ketamine antidepressant responses in female rodents compared to males[20,21], we observed greater antidepressant potency of ketamine in female mice in the FST (Fig. 2b), which was not associated with sex differences in ketamine-induced hyperlocomotion (probably mediated by NMDAR inhibition[22]; Extended Data Fig. 4a, b). To investigate whether these sex-dependent antidepressant differences are explained by a different pharmacokinetic profile of ketamine in males versus females, we measured the levels of ketamine and its metabolites in the brains of mice after ketamine administration. While equivalent levels of ketamine and norketamine were found, (2*S*,6*S*;2*R*,6*R*)-HNK was approximately three-fold higher in the brains of female mice compared to males (Fig. 2c–e), suggesting a role of (2*S*,6*S*;2*R*,6*R*)-HNK in the antidepressant effects of ketamine. To directly determine

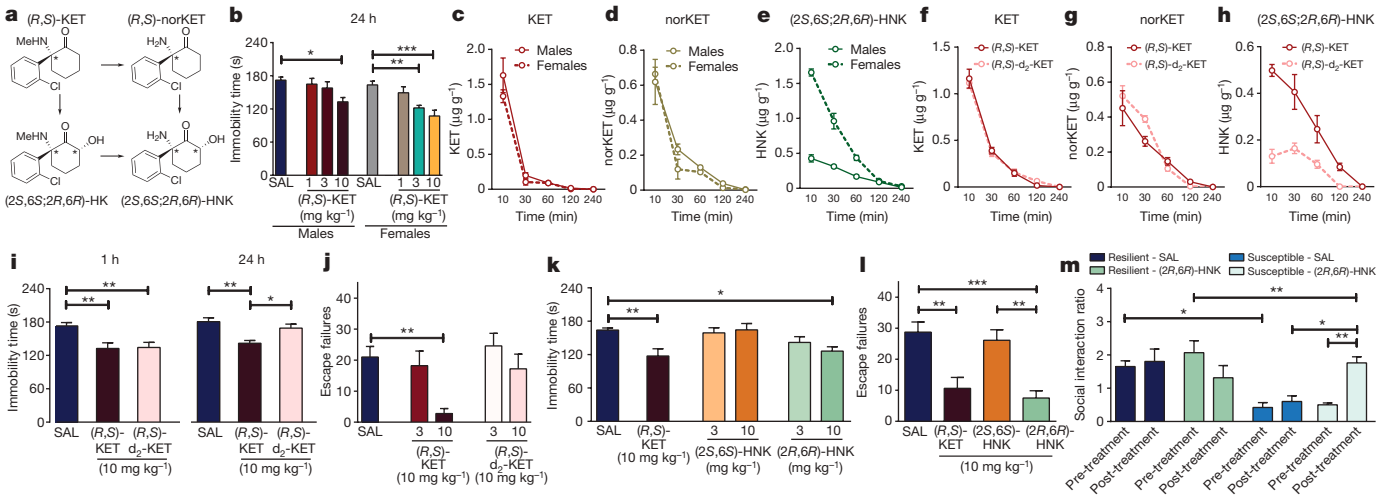

Figure 2 | Metabolism of ketamine to (2*R*,6*R*)-HNK is necessary and sufficient to exert antidepressant actions. a, Simplified diagram of (*R*,*S*)-KET metabolism. **b**–**e**, Greater antidepressant-like actions of ketamine in female mice compared to males in the FST (**b**) are associated with higher brain levels of (2*S*,6*S*;2*R*,6*R*)-HNK (**e**), but not KET (**c**) or norketamine (norKET) (**d**). **f**–**h**, Brain levels of KET (**f**), norKET (**g**) and (2*S*,6*S*;2*R*,6*R*)-HNK (**h**) after administration of (*R*,*S*)-KET and 6,6-dideuteroketamine ((*R*,*S*)-d_2-KET). **i**, **j**, Effects of (*R*,*S*)-KET and (*R*,*S*)-d_2-KET in the 1-h and 24-h FST (**i**) and the learned helplessness test (**j**). **k**, **l**, Compared to (2*S*,6*S*)-HNK, (2*R*,6*R*)-HNK manifested greater potency and longer-lasting antidepressant-like effects in the FST (**k**) and learned helplessness test (**l**). **m**, (2*R*,6*R*)-HNK reversed chronic social defeat-induced social interaction deficits. Data are mean ± s.e.m. $*P < 0.05$, $**P < 0.01$, $***P < 0.001$ (see Supplementary Table 1 for statistical analyses and *n* numbers).

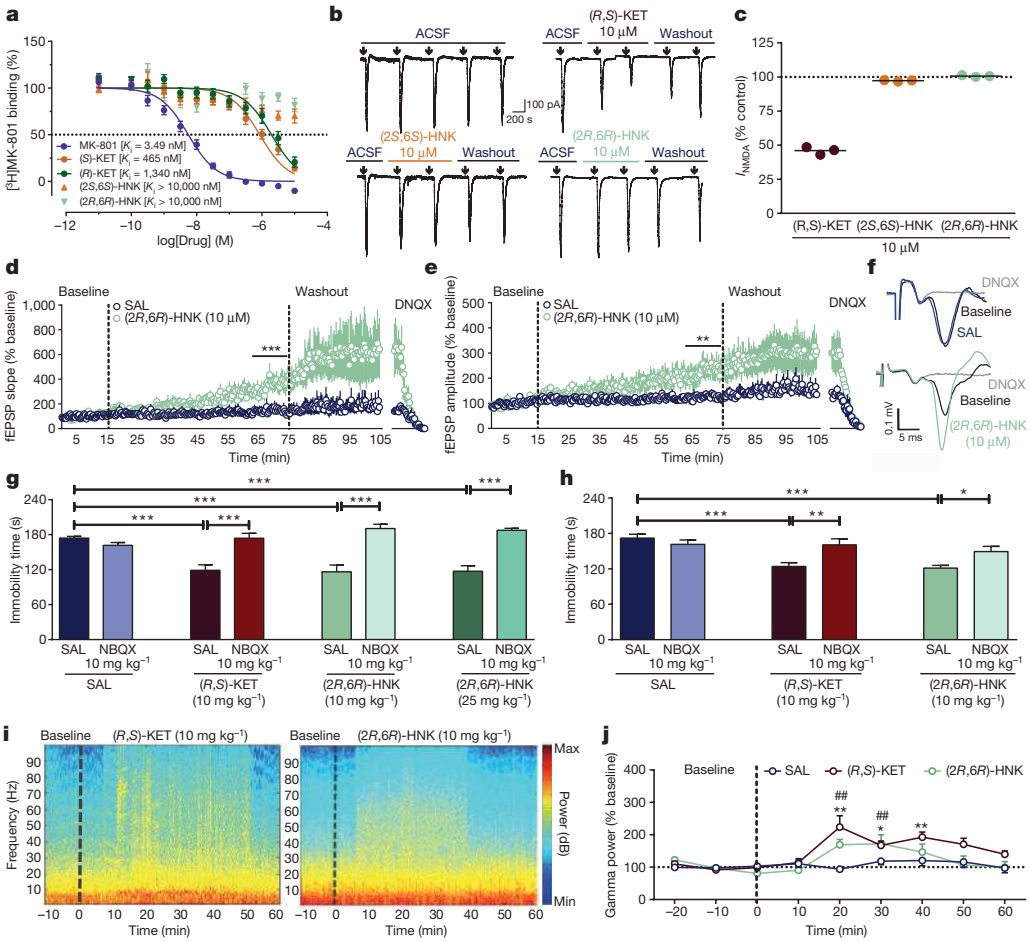

Figure 3 | Role of NMDA and AMPA glutamate receptors in the acute antidepressant effects of (2*R*,6*R*)-HNK. a, (2*R*,6*R*)-HNK does not displace [^{3}H]MK-801 binding. **b**, **c**, (*R*,*S*)-KET inhibited, but (2*S*,6*S*)-HNK and (2*R*,6*R*)-HNK did not inhibit currents evoked by application of NMDA to stratum radiatum interneurons in rat hippocampal slices (**b**), quantified as percentage inhibition (I_{NMDA}; **c**). Arrows indicate 30-s agonist pulse. ACSF, artificial cerebrospinal fluid. **d**, **e**, Normalized fEPSP slope (**d**) and amplitude (**e**) from stimulation of the Schaffer collateral pathway in rat hippocampal slices. **f**, Representative field-potential traces in the same hippocampal slice before (baseline) and 60 min after application of SAL or (2*R*,6*R*)-HNK. **g**, **h**, Pre-treatment with the AMPAR inhibitor NBQX 10 min before (*R*,*S*)-KET or (2*R*,6*R*)-HNK prevented their antidepressant-like actions in the 1-h (**g**) or 24-h (**h**) FST. **i**, Representative qEEG spectrograms for 10-min before (baseline) and 1-h after administration of (*R*,*S*)-ketamine or (2*R*,6*R*)-HNK (indicated by a dashed line). **j**, Normalized gamma power changes after administration of (*R*,*S*)-KET, (2*R*,6*R*)-HNK or vehicle (SAL). Data are mean ± s.e.m. $^*P < 0.05$, $^{**}P < 0.01$, $^{***}P < 0.001$; in **j**, * denotes (*R*,*S*)-KET, # denotes (2*R*,6*R*)-HNK (see Supplementary Table 1 for statistical analyses and *n* numbers).

whether metabolism of ketamine to (2*S*,6*S*;2*R*,6*R*)-HNK is required for its antidepressant actions, we deuterated ketamine at the C6 position (6,6-dideuteroketamine; (R,S)-d_2-KET, Extended Data Fig. 2f). This alteration would not change the pharmacological properties of unmetabolized ketamine, but may change the relative rate of metabolism[23]. Indeed, 6,6-dideuteroketamine did not change NMDAR binding affinity (Extended Data Fig. 2g), or NMDAR-mediated hyperlocomotion (Extended Data Fig. 4c, d), but robustly hindered its metabolism to (2*S*,6*S*;2*R*,6*R*)-HNK, without changing the ketamine levels in the brain (Fig. 2f–h). Unlike ketamine, administration of 6,6-dideuteroketamine did not induce antidepressant actions in the FST (Fig. 2i) or learned helplessness test (Fig. 2j) 24 h after administration, indicating a role of (2*S*,6*S*;2*R*,6*R*)-HNK in the sustained antidepressant effects. Notably, published human data reveal a positive correlation between the antidepressant responses of ketamine and plasma (2*S*,6*S*;2*R*,6*R*)-HNK metabolite levels[19].

To determine whether (2*S*,6*S*)-HNK or (2*R*,6*R*)-HNK exert antidepressant effects independently of ketamine administration, we compared their behavioural effects in the 24-h (sustained) FST and learned helplessness test. We observed more potent antidepressant effects after administration of the (2*R*,6*R*)-HNK metabolite (Fig. 2k, l), which is exclusively derived from (*R*)-ketamine, and thus consistent with the greater antidepressant actions of (*R*)-ketamine relative to (*S*)-ketamine (Fig. 1b–d). Moreover, (2*R*,6*R*)-HNK resulted in a dose-dependent antidepressant action in the learned helplessness test, FST and NSF test (Extended Data Fig. 5a, c, f). We note that (2*S*,6*S*)-HNK also exerts antidepressant actions at higher doses (Extended Data Fig. 5b, d). The greater antidepressant effects of (2*R*,6*R*)-HNK do not result from higher brain levels of the drug compared to (2*S*,6*S*)-HNK (Extended Data Fig. 5e). Similar to ketamine, a single (2*R*,6*R*)-HNK administration induced persistent antidepressant effects in the FST, lasting for at least 3 days (Extended Data Fig. 5g). A single (2*R*,6*R*)-HNK administration also reversed chronic corticosterone-induced anhedonia assessed with the sucrose preference and female urine sniffing behavioural tasks (Extended Data Fig. 5h, i), as well as social avoidance induced by chronic social defeat stress (Fig. 2m; Extended Data Fig. 5j, k).

(2*R*,6*R*)-HNK effects on glutamate receptors

A prominent hypothesis for the mechanism of action of ketamine is that it acts via direct inhibition of NMDARs localized to interneurons. This is suggested to lead to disinhibition of glutamatergic neurons, which receive input from interneurons, and a resultant rapid increase in glutamate synaptic transmission in mood-relevant brain regions[24]. However, in contrast to ketamine, (2*R*,6*R*)-HNK does not displace [^{3}H]MK-801 binding to the NMDAR *in vitro* (Fig. 3a; also see ref. 12) and does not functionally inhibit NMDARs localized to stratum radiatum interneurons in hippocampal slices (Fig. 3b, c). Instead, (2*R*,6*R*)-HNK induced a robust increase in AMPAR-mediated excitatory post-synaptic potentials (EPSPs) recorded from the CA1 region of hippocampal slices after stimulation of Schaffer collateral axons, which was sustained after washout of the drug (Fig. 3d–f). (2*R*,6*R*)-HNK also increased the frequency and amplitude of AMPAR-mediated excitatory postsynaptic currents (EPSCs) recorded from CA1 stratum radiatum interneurons (Extended Data Fig. 6a–j), which receive glutamatergic inputs from the Schaffer collaterals. To test the extent to which the antidepressant effect of (2*R*,6*R*)-HNK depends on AMPAR activation *in vivo*, mice were pre-treated with the AMPAR antagonist 2, 3-dihydroxy-6-nitro-7-sulfamoyl-benzo[f]quinoxaline-2, 3-dione (NBQX) 10 min before treatment with ketamine or (2*R*,6*R*)-HNK. Mice were then assessed in the FST 1 or 24 h after the treatment.

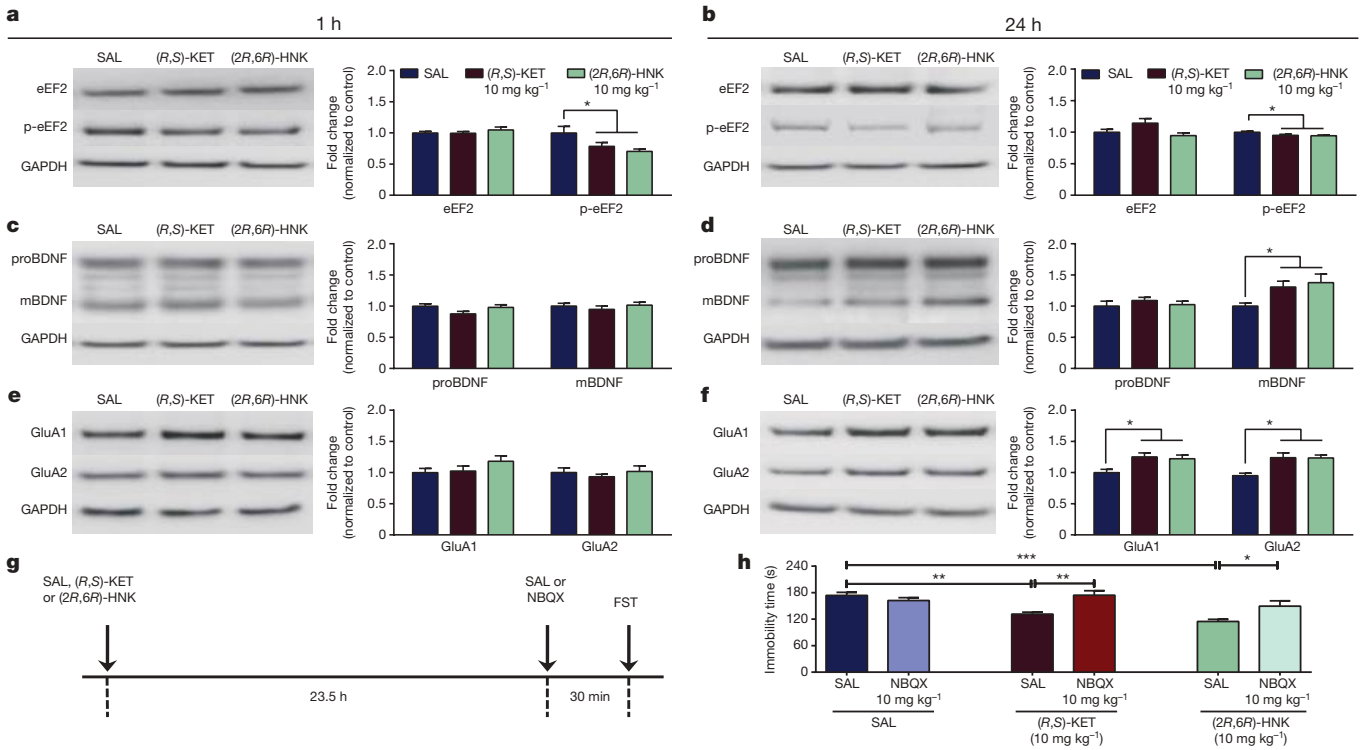

Figure 4 | Role of AMPARs in the sustained antidepressant effects of (2*R*,6*R*)-HNK. a–h, Protein and protein phosphorylation levels from hippocampal synaptoneurosomes. **a**, **b**, A single administration of (*R*,*S*)-KET or (2*R*,6*R*)-HNK decreased phosphorylation of eEF2 (p-eEF2), 1 h (**a**) and 24 h (**b**) after injection. **c**, **d**, Although administration of (2*R*,6*R*)-HNK or (*R*,*S*)-KET did not alter the levels of proBDNF or mature BDNF (mBDNF) 1 h after injection (**c**), it increased mBDNF levels 24 h after treatment (**d**). **e**, **f**, (*R*,*S*)-KET and (2*R*,6*R*)-HNK did not change GluA1 and GluA2 levels at 1 h after treatment (**e**), but did increase levels 24 h after injection (**f**). **g**, **h**, Administration of the AMPAR inhibitor NBQX 30 min before the 24-h FST prevented the antidepressant effects of both (*R*,*S*)-KET and (2*R*,6*R*)-HNK administered 23.5 h before NBQX. Data are mean ± s.e.m. Images cropped; see Supplementary Fig. 1 for complete blot images. GAPDH was used as a loading control. $*P < 0.05$, $**P < 0.01$, $***P < 0.001$ (see Supplementary Table 1 for statistical analyses and *n* numbers).

Similar NBQX treatment has previously been shown to prevent the antidepressant actions of ketamine, without affecting other behaviours in rodents[15,25–27]. Treatment with NBQX, prior to (2*R*,6*R*)-HNK, prevented both the 1-h and 24-h antidepressant effects of (2*R*,6*R*)-HNK (Fig. 3g, h), indicating that its antidepressant actions require the acute activation of AMPARs.

A non-invasive method used to assess ketamine-activated circuitry in both humans and rodents is the quantitative electroencephalography (qEEG) measurement of gamma-band power, which is dependent on activation of fast ionotropic excitatory receptors, including AMPARs[28–30]. We show that, similar to ketamine, (2*R*,6*R*)-HNK administration acutely increases gamma power measured via surface electrodes *in vivo* (Fig. 3i, j), independent of locomotor activity changes, and without altering alpha, beta, delta or theta oscillations (Extended Data Fig. 7a–e). Importantly, pre-treatment with NBQX prevented (2*R*,6*R*)-HNK-induced increases in gamma power, thus further implicating AMPARs in the (2*R*,6*R*)-HNK mechanism of action (Extended Data Fig. 7f–k), and validating a potential human translational biomarker of the central nervous system response to (2*R*,6*R*)-HNK.

Evidence indicates that mammalian target of rapamycin (mTOR) signalling[25], protein synthesis through eukaryotic translation elongation factor 2 (eEF2) dephosphorylation[16], as well as brain-derived neurotrophic factor (BDNF) increases[16,31], underlie the antidepressant responses of ketamine. We examined whether administration of (2*R*,6*R*)-HNK affects phosphorylation of mTOR (Ser2448) and eEF2 (Thr56), or BDNF levels in synaptoneurosome fractions of the hippocampus and prefrontal cortex. No differences were observed in mTOR phosphorylation after administration of ketamine or (2*R*,6*R*)-HNK in the hippocampus or prefrontal cortex of mice (Extended Data Fig. 8a–d). However, ketamine induced a decrease in eEF2 phosphorylation in the hippocampus 1 h and 24 h after injection, and increased hippocampal BDNF at 24 h (Fig. 4a–d). These changes did not occur in the prefrontal cortex (Extended Data Fig. 8e–h), but were recapitulated by (2*R*,6*R*)-HNK administration (Fig. 4a–d), and may be partially responsible for its sustained antidepressant actions.

It is noteworthy that (2*R*,6*R*)-HNK resulted in antidepressant actions (Fig. 2k–m; Extended Data Fig. 5) at time points (for example, 24 h) past when its brain concentrations are below detectable levels (for example, 2 h; Extended Data Fig. 5e). Synaptic plasticity changes involving AMPARs are thought to underlie such long-term antidepressant actions of ketamine[24,27]. Here we show that while neither ketamine nor (2*R*,6*R*)-HNK administration altered the levels of AMPAR subunits GluA1 and GluA2 in hippocampal synaptoneurosomes 1 h after treatment (Fig. 4e), they both increased GluA1 and GluA2 levels 24 h after treatment in mouse hippocampal (Fig. 4f), but not prefrontal cortex synaptoneurosomes (Extended Data Fig. 8i, j). Consistent with an increase in synaptic AMPARs being involved in the sustained, 24-h, antidepressant actions, administration of NBQX 30 min prior to the 24-h FST (23.5 h after antidepressant treatment; see timeline Fig. 4g) prevented the antidepressant actions of both ketamine and (2*R*,6*R*)-HNK (Fig. 4h). These findings implicate an AMPAR-mediated maintenance of synaptic potentiation to underlie the sustained antidepressant effects of (2*R*,6*R*)-HNK.

(2*R*,6*R*)-HNK lacks ketamine-related side effects

Ketamine has abuse potential, as well as sensory-dissociation properties and other side effects, which limit its potential widespread use for the treatment of depression[9]. While administration of ketamine (Extended Data Fig. 4a–d) and (2*S*,6*S*)-HNK (Fig. 5a) were associated with increased locomotor activity and motor incoordination (Fig. 5c, d), (2*R*,6*R*)-HNK did not induce any significant changes in locomotion, and did not affect coordination as measured by the accelerating rotarod test (Fig. 5b, d). We show that unlike ketamine, (2*R*,6*R*)-HNK

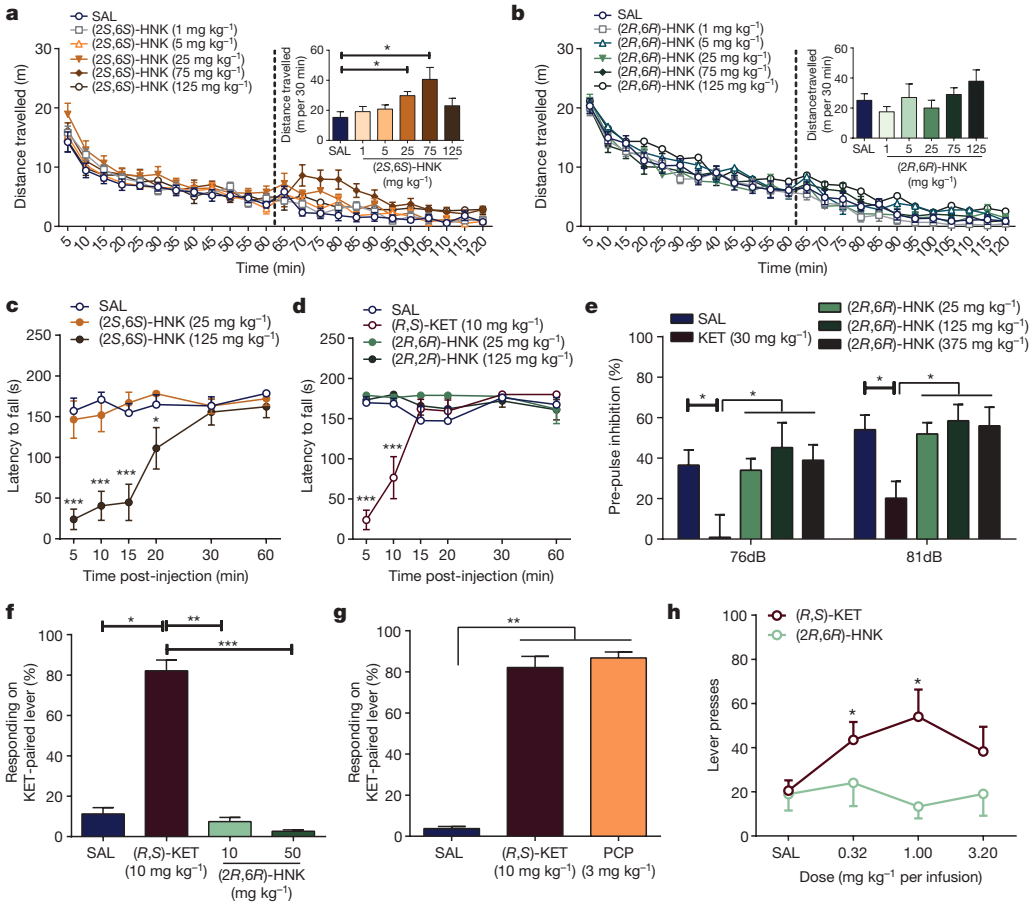

Figure 5 | (2*R*,6*R*)-HNK lacks side effects of ketamine. **a**, **b**, After recording baseline activity for 1 h, mice received drug (dashed line) and locomotor activity was monitored for 1 h. Administration of (2*S*,6*S*) HNK dose-dependently changed locomotor activity (**a**), whereas administration of (2*R*,6*R*)-HNK did not (**b**). **c**, **d**, (2*S*,6*S*)-HNK (**c**) but not (2*R*,6*R*)-HNK (**d**) induced motor in-coordination in the rotarod. **e**–**h**, Unlike (*R*,*S*)-KET, (2*R*,6*R*)-HNK administration did not induce pre-pulse inhibition deficits (**e**), (*R*,*S*)-KET-associated discriminative stimulus (**f**, **g**), or self-administration (**h**). Data are mean ± s.e.m. $*P < 0.05$, $**P < 0.01$, $***P < 0.001$ (see Supplementary Table 1 for statistical analyses and *n* numbers).

administration, even at high doses (375 mg kg^{-1}), did not affect sensory gating as assessed with pre-pulse inhibition (Fig. 5e) or startle amplitude (Extended Data Fig. 9a). Non-competitive NMDAR antagonists, including ketamine and phencyclidine, produce discriminative stimulus effects in drug discrimination protocols and manifest cross-drug substitution profiles at an antidepressant-relevant dose range[32]. In ketamine-trained mice, (2*R*,6*R*)-HNK administration did not produce ketamine-related discrimination responses, whereas phencyclidine (PCP) did (Fig. 5f, g), without either of these drugs changing overall lever pressing response rates (Extended Data Fig. 9b, c). These findings further support a non-NMDAR mechanism for (2*R*,6*R*)-HNK action including interoceptive effects, unlike the abused drugs ketamine and PCP. Since drug discrimination does not independently predict abuse potential per se, we further assessed the effects of ketamine and (2*R*,6*R*)-HNK in an intravenous drug self-administration model, classically used for the evaluation of abuse/addiction liability. Intravenous ketamine was readily self-administered and resulted in a significant increase in drug intake (Fig. 5h; Extended Data Fig. 9d). By contrast, mice did not self-administer pharmacologically relevant doses of (2*R*,6*R*)-HNK under the same conditions (Fig. 5h; Extended Data Fig. 9d). Overall, (2*R*,6*R*)-HNK administration revealed an innocuous side-effect profile compared to ketamine.

Discussion

Our data provide new evidence explaining the unique antidepressant effects of ketamine and implicate an NMDAR inhibition-independent mechanism. These findings reveal that production of a distinct metabolite of ketamine is necessary and sufficient to produce the ketamine antidepressant actions. Overall, our data indicate that administration of (2*R*,6*R*)-HNK induces an acute increase in glutamatergic signalling (as supported by our EPSP, EPSC and qEEG measurements), followed by a long-term adaptation involving the upregulation of synaptic AMPARs, as evidenced by an increase in GluA1 and GluA2 in hippocampal synapses. This is supported by the finding that NBQX reverses both the acute (delivered before (2*R*,6*R*)-HNK) (Fig. 3g, h) and sustained (delivered after (2*R*,6*R*)-HNK; Fig. 4g, h) antidepressant actions of (2*R*,6*R*)-HNK. Considering the lack of side effects, and the favourable physiochemical properties of HNKs[33], these findings have relevance for the development of next-generation, rapid-acting antidepressants.

Online Content Methods, along with any additional Extended Data display items and Source Data, are available in the online version of the paper; references unique to these sections appear only in the online paper.

Received 15 October 2015; accepted 12 April 2016.
Published online 4 May 2016.

1. Kessler, R.C. *et al.* The epidemiology of major depressive disorder: results from the National Comorbidity Survey Replication (NCS-R). *JAMA* **289,** 3095–3105 (2003).
2. Trivedi, M. H. *et al.* Evaluation of outcomes with citalopram for depression using measurement-based care in STAR*D: implications for clinical practice. *Am. J. Psychiatry* **163,** 28–40 (2006).
3. Rush, A. J. *et al.* Acute and longer-term outcomes in depressed outpatients requiring one or several treatment steps: a STAR*D report. *Am. J. Psychiatry* **163,** 1905–1917 (2006).
4. Zarate, C. A., Jr *et al.* A randomized trial of an N-methyl-D-aspartate antagonist in treatment-resistant major depression. *Arch. Gen. Psychiatry* **63,** 856–864 (2006).
5. Berman, R. M. *et al.* Antidepressant effects of ketamine in depressed patients. *Biol. Psychiatry* **47,** 351–354 (2000).
6. Diazgranados, N. *et al.* A randomized add-on trial of an *N*-methyl-D-aspartate antagonist in treatment-resistant bipolar depression. *Arch. Gen. Psychiatry* **67,** 793–802 (2010).
7. Lally, N. *et al.* Anti-anhedonic effect of ketamine and its neural correlates in treatment-resistant bipolar depression. *Transl. Psychiatry* **4,** e469 (2014).
8. Murrough, J. W. *et al.* Antidepressant efficacy of ketamine in treatment-resistant major depression: a two-site randomized controlled trial. *Am. J. Psychiatry* **170,** 1134–1142 (2013).
9. Morgan, C. J. & Curran, H. V. Ketamine use: a review. *Addiction* **107,** 27–38 (2012).
10. Newport, D. J. *et al.* Ketamine and other NMDA antagonists: early clinical trials and possible mechanisms in depression. *Am. J. Psychiatry* **172,** 950–966 (2015).

11. Leung, L. Y. & Baillie, T. A. Comparative pharmacology in the rat of ketamine and its two principal metabolites, norketamine and (*Z*)-6-hydroxynorketamine. *J. Med. Chem.* **29,** 2396–2399 (1986).
12. Moaddel, R. *et al.* Sub-anesthetic concentrations of (*R,S*)-ketamine metabolites inhibit acetylcholine-evoked currents in α7 nicotinic acetylcholine receptors. *Eur. J. Pharmacol.* **698,** 228–234 (2013).
13. Ebert, B., Mikkelsen, S., Thorkildsen, C. & Borgbjerg, F. M. Norketamine, the main metabolite of ketamine, is a non-competitive NMDA receptor antagonist in the rat cortex and spinal cord. *Eur. J. Pharmacol.* **333,** 99–104 (1997).
14. Yang, C. *et al.* R-ketamine: a rapid-onset and sustained antidepressant without psychotomimetic side effects. *Transl. Psychiatry* **5,** e632 (2015).
15. Maeng, S. *et al.* Cellular mechanisms underlying the antidepressant effects of ketamine: role of α-amino-3-hydroxy-5-methylisoxazole-4-propionic acid receptors. *Biol. Psychiatry* **63,** 349–352 (2008).
16. Autry, A. E. *et al.* NMDA receptor blockade at rest triggers rapid behavioural antidepressant responses. *Nature* **475,** 91–95 (2011).
17. Desta, Z. *et al.* Stereoselective and regiospecific hydroxylation of ketamine and norketamine. *Xenobiotica* **42,** 1076–1087 (2012).
18. Adams, J. D., Jr, Baillie, T. A. & Trevor, A. J. & Castagnoli, N. Jr. Studies on the biotransformation of ketamine. 1-Identification of metabolites produced *in vitro* from rat liver microsomal preparations. *Biomed. Mass Spectrom.* **8,** 527–538 (1981).
19. Zarate, C. A., Jr *et al.* Relationship of ketamine's plasma metabolites with response, diagnosis, and side effects in major depression. *Biol. Psychiatry* **72,** 331–338 (2012).
20. Carrier, N. & Kabbaj, M. Sex differences in the antidepressant-like effects of ketamine. *Neuropharmacology* **70,** 27–34 (2013).
21. Franceschelli, A., Sens, J., Herchick, S., Thelen, C. & Pitychoutis, P. M. Sex differences in the rapid and the sustained antidepressant-like effects of ketamine in stress-naive and "depressed" mice exposed to chronic mild stress. *Neuroscience* **290,** 49–60 (2015).
22. Irifune, M., Shimizu, T., Nomoto, M. & Fukuda, T. Involvement of *N*-methyl-D-aspartate (NMDA) receptors in noncompetitive NMDA receptor antagonist-induced hyperlocomotion in mice. *Pharmacol. Biochem. Behav.* **51,** 291–296 (1995).
23. Gant, T. G. Using deuterium in drug discovery: leaving the label in the drug. *J. Med. Chem.* **57,** 3595–3611 (2014).
24. Duman, R. S., Aghajanian, G. K., Sanacora, G. & Krystal, J. H. Synaptic plasticity and depression: new insights from stress and rapid-acting antidepressants. *Nature Med.* **22,** 238–249 (2016).
25. Li, N. *et al.* mTOR-dependent synapse formation underlies the rapid antidepressant effects of NMDA antagonists. *Science* **329,** 959–964 (2010).
26. Koike, H., Iijima, M. & Chaki, S. Involvement of AMPA receptor in both the rapid and sustained antidepressant-like effects of ketamine in animal models of depression. *Behav. Brain Res.* **224,** 107–111 (2011).
27. Koike, H. & Chaki, S. Requirement of AMPA receptor stimulation for the sustained antidepressant activity of ketamine and LY341495 during the forced swim test in rats. *Behav. Brain Res.* **271,** 111–115 (2014).
28. Whittington, M. A., Traub, R. D., Kopell, N., Ermentrout, B. & Buhl, E. H. Inhibition-based rhythms: experimental and mathematical observations on network dynamics. *Int. J. Psychophysiol.* **38,** 315–336 (2000).
29. Cunningham, M. O., Davies, C. H., Buhl, E. H., Kopell, N. & Whittington, M. A. Gamma oscillations induced by kainate receptor activation in the entorhinal cortex *in vitro*. *J. Neurosci.* **23,** 9761–9769 (2003).
30. Muthukumaraswamy, S. D. *et al.* Evidence that Subanesthetic doses of ketamine cause sustained disruptions of NMDA and AMPA-mediated frontoparietal connectivity in humans. *J. Neurosci.* **35,** 11694–11706 (2015).
31. Lepack, A. E., Fuchikami, M., Dwyer, J. M., Banasr, M. & Duman, R. S. BDNF release is required for the behavioral actions of ketamine. *Int. J. Neuropsychopharmacol.* **18,** pyu033 (2015).
32. De Vry, J. & Jentzsch, K. R. Role of the NMDA receptor NR2B subunit in the discriminative stimulus effects of ketamine. *Behav. Pharmacol.* **14,** 229–235 (2003).
33. Moaddel, R. *et al.* The distribution and clearance of (2*S*,6*S*)-hydroxynorketamine, an active ketamine metabolite, in Wistar rats. *Pharmacol. Res. Perspect.* **3,** e00157 (2015).

Supplementary Information is available in the online version of the paper.

Acknowledgements We thank A. Keller for his assistance with the qEEG experiments, M. K. Lobo for assistance with the social defeat experiments, B. Alkondon for the rat hippocampal slice preparation and biocytin processing, V. Meadows and S. Krimmel for assistance with behavioural experiments and manuscript review, E. Pereira for critical comments on the manuscript and figures, D. Luckenbaugh for assistance with statistical analysis, and C. Moore for the small molecule X-ray crystallography. Research was supported by NIMH grants MH099345 and MH107615 to T.D.G. and MH086828 to S.M.T., and the NIA (R.M., I.W.W.), NIMH (C.A.Z.), and NCATS (C.J.T.) NIH intramural research programs. Receptor binding profiles and K_i determinations were supported by the NIMH Psychoactive Drug Screening Program, Contract HHSN-271-2008-025C, to B. L. Roth in conjunction with J. Driscoll. Initial synthesis of the ketamine metabolites used in this study was supported by NIA Contract HHSN271201000008I to I.W.W.

Author Contributions P.Z., R.M., P.J.M., I.W.W., C.J.T., C.A.Z. and T.D.G. were responsible for the overall experimental design. P.J.M., Y.F. and C.J.T. synthesised the ketamine metabolites and deuterated ketamine derivatives, and provided mass spectrometer confirmations. Bioanalytical quantitation of ketamine and metabolites were performed by R.M., N.S.S. and K.S.S.D.. P.Z., P.G. and H.J.P. conducted and analysed the results of the behavioural and qEEG experiments. X.-P.H. supervised and analysed the results of the binding experiments. P.Y. performed the western blot experiments. E.X.A., M.A., J.F. and S.M.T. helped design and analyse the electrophysiology experiments, which were conducted by M.A., J.F. and S.M.T. G.I.E. and C.L.M. conducted and analysed the results of the i.v. self-administration. P.Z. and T.D.G. outlined and wrote the paper, which was reviewed by all authors.

Author Information Reprints and permissions information is available at www.nature.com/reprints. The authors declare competing financial interests: details are available in the online version of the paper. Readers are welcome to comment on the online version of the paper. Correspondence and requests for materials should be addressed to T.D.G. (gouldlab@me.com).

METHODS

Animals. Mice and rats were acclimated to University of Maryland, Baltimore, vivarium for at least 7 days before experiments. Food and water were available *ad libitum*. CD-1 mice (males unless otherwise noted; 8–10 weeks old; Charles River Laboratories) were housed in groups of 4–5 per cage with a constant 12-h light/dark cycle (lights on/off at 07:00/19:00). For the social defeat experiments, 8–9-week-old male C57BL/6J mice (University of Maryland, Baltimore, veterinary resources breeding colony) and retired male CD-1 breeders (Charles River Laboratories) were used. For the whole-cell and field potential electrophysiological recordings, male Sprague–Dawley rats (postnatal day 24–35; Charles River) were used. All experimental procedures were approved by the University of Maryland, Baltimore Animal Care and Use Committee and were conducted in full accordance with the National Institutes of Health Guide for the Care and Use of Laboratory Animals.

Drugs. (*R*,*S*)-ketamine, (*S*)-ketamine, desipramine, MK-801, PCP (Sigma-Aldrich), (*R*)-ketamine (Cayman Chemicals) and NBQX (National Institute of Mental Health Chemical Synthesis and Drug Supply Program) were dissolved in 0.9% saline. (2*S*,6*S*)-HNK, (2*R*,6*R*)-HNK and 6,6-dideuteroketamine hydrochloride were synthesized and characterized both internally at the National Center for Advancing Translational Sciences and at SRI International as described in Supplementary Information. Absolute and relative stereochemistry for (2*S*,6*S*)-HNK and (2*R*,6*R*)-HNK were confirmed by small molecule X-ray crystallography, as described in the Supplementary Information.

All drugs were dissolved in 0.9% saline, and administered intraperitoneally (i.p.) in a volume of 7.5 ml kg^{-1} of body mass by a male experimenter for the behavioural studies. Corticosterone (4-pregnen-11β, 21-diol-3, 20-dione 21-hemisuccinate; Steraloids) was dissolved in tap water. For the electrophysiology recordings, test drugs were diluted in ACSF.

FST. Mice were tested in the FST 1 h and/or 24 h after injection. During the test, mice were subjected to a 6-min swim session in clear Plexiglass cylinders (30 cm height × 20 cm diameter) filled with 15 cm of water (23 ± 1 °C). The test was performed in normal light conditions (800 Lx). Sessions were recorded using a digital video camera. Immobility time, defined as passive floating with no additional activity other than that necessary to keep the animal's head above the water, was scored for the last 4 min of the 6-min test by a trained observer.

We conducted three different FST experiments where we used the AMPAR antagonist NBQX. In the first two experiments, we administered NBQX 10 min before ketamine, (2*R*,6*R*)-hydroxynorketamine, or vehicle and then tested the mice 1 h and 24 h later to assessed whether AMPAR activity is necessary for the acute actions of these drugs, leading to both acute and sustained antidepressant effects. In the third experiment we first administered ketamine, (2*R*,6*R*)-HNK, or vehicle and 23.5 h later mice received either NBQX or vehicle. Thirty minutes later we tested these mice in the FST, to assess effects of AMPAR activity on sustained antidepressant actions.

Open-field test. Mice were placed into individual open-field arenas (50 × 50 × 38 cm (length × width × height); San Diego Instruments) for a 60-min habituation period. Mice then received an injection of the respective drug and assessed for locomotor activity for another 60 min. Distance travelled was analysed using TopScan v2.0 (CleverSys, Inc.).

NSF test. Mice were singly housed and food-deprived for 24 h in freshly made home-cages. Two normal chow diet pellets were placed on an inverted weighing-boat platform (10 × 10 × 1.5 cm) in the centre of an open-field arena (40 × 40 cm). Thirty or sixty minutes (see figure legends) after drug administration, mice were introduced into a corner of the arena. The time needed for the mice to take a bite of food was recorded over a 10-min period by a trained observer. After the test, the mice were returned to their home cage containing pre-weighed food pellets, and latency to start biting the pellet, as well as consumption was recorded for a period of 10 min. There was no significant change in home cage latency or consumption in any of our experiments (data not shown).

Learned helplessness test. The learned helplessness model consisted of three different phases: inescapable shock training, learned helplessness screening, and the test. For the inescapable shock portion of the test (day 1), the animals were placed in one side of two-chambered shuttle boxes (34 × 37 × 18 cm (height × width × depth); Coulbourn Instruments), with the door between the chambers closed. After a 5-min adaptation period, 120 inescapable foot-shocks (0.45 mA, 15 s duration, randomized average inter-shock interval of 45 s) were delivered through the floor. During the screening session (day 2), the mice were placed in one of the two chambers of the apparatus for 5 min. A shock (0.45 mA) was then delivered, and the door between the two chambers was raised simultaneously. Crossing over into the second chamber terminated the shock. If the animal did not cross over, the shock terminated after 3 s. A total of 30 screening trials of escapable shocks were presented to each mouse with an average of 30-s delay between each trial. Mice that developed helplessness behaviour (>5 escape failures during the last 10 screening shocks) received the assigned drug 24 h after screening (day 3). During the learned helplessness test phase (day 4), the animals were placed in the shuttle boxes and, after a 5-min adaptation period, a 0.45-mA shock was delivered concomitantly with door opening for the first five trials, followed by a 2-s delay for the next 40 trials. Crossing over to the second chamber terminated the shock. If the animal did not cross over to the other chamber, the shock was terminated after 24 s. A total of 45 trials of escapable shocks were presented to each mouse with 30-s inter-trial intervals. The number of escape failures was recorded for each mouse by automated computer software (Graphic State v3.1; Coulbourn Instruments).

Chronic social defeat stress and social interaction. The timeline for the social defeat experiments is presented in Extended Data Fig. 3a. Male C57BL/6J mice underwent a 10-day chronic social defeat stress model, as described elsewhere[34], with some modifications. In brief, experimental mice were introduced to the home cage (43 × 11 × 20 cm (length × width × height)) of a resident aggressive retired CD-1 breeder, pre-screened for aggressive behaviours, for 10 min. After this physical attack phase, mice were transferred and housed in the opposite side of the resident's cage divided by a Plexiglas perforated divider, to maintain continuous sensory contact. This process was repeated for 10 days. Experimental mice were introduced to a novel aggressive CD-1 mouse each day. On day 11, test mice were screened for susceptibility in a social interaction/avoidance choice test. The social interaction apparatus consisted of a rectangular three-chambered box (mouse conditioned-place preference chamber; Stoelting Co., see Extended Data Fig. 3b) containing two equal sized end-chambers and a smaller central chamber. The social interaction/avoidance choice test consisted of two 5-min phases. During the habituation phase, mice explored the empty apparatus. During the test phase, two small wire cages (Galaxy Cup, Spectrum Diversified Designs, Inc.), one containing a 'stranger' CD-1 mouse and the other one empty, were placed in the far corners of each chamber. The time spent interacting (nose within close proximity of the cage) with the stranger mouse versus the empty cage was analysed using TopScan video tracking software (CleverSys). Locomotor activity (total distance moved over 5 min) and number of total crosses into and out of the central chamber were also measured. The social interaction ratio was calculated by dividing the time spent interacting with the stranger by the time spent with the empty cage. Mice having a social interaction ratio higher than 1.0 were considered resilient, and mice with a social interaction ratio lower than 1.0 were considered susceptible. On day 13 resilient and susceptible mice received an i.p. injection of saline, (*R*,*S*)-KET (20 mg kg^{-1}; chosen based on dose previously effective in C57BL/6J mice[34]), MK-801 (0.1 mg kg^{-1}) or (2*R*,6*R*)-HNK (20 mg kg^{-1}). Mice were re-tested for social interaction/avoidance on day 15 (24 h after treatment).

Chronic corticosterone-induced anhedonia. *Sucrose preference test.* For assessing the baseline sucrose preference, mice were singly housed for 24 h and presented with two identical bottles containing either tap water or 1% sucrose solution. After baseline sucrose measurement, mice were re-group housed (5 mice per cage) and treated for 4 weeks with corticosterone (25 μg ml^{-1} equivalent) given in water bottles. Before initiation of any behavioural measurements, animals were weaned off corticosterone treatment; 3 days corticosterone 12.5 μg ml^{-1} and 3 days corticosterone 6.25 μg ml^{-1}, followed by 1 week of complete withdrawal. Mice were subsequently singly housed in freshly made home cages and provided with two bottles containing either tap water or 1% sucrose solution. Twenty-four hours later, mice that developed the anhedonia phenotype (<70% sucrose preference) were treated with saline or (2*R*,6*R*)-HNK (10 mg kg^{-1}) and sucrose preference was measured after an additional 24 h.

Female urine sniffing test. A separate cohort of mice was treated with the same chronic corticosterone administration model as described above but assessed for female urine sniffing preference as a measure of hedonic behaviour[35]. Mice were singly housed in freshly made home cages for a habituation period of 10 min. Subsequently, one plain cotton tip was secured on the centre of the cage wall and mice were allowed to sniff and habituate to the tip for a period of 30 min. Then, the plain cotton tip was removed and replaced by two cotton tip applicators, one infused with fresh female mouse oestrus urine and the other with fresh male mouse urine. These applicators were presented and secured at the two corners of the cage wall simultaneously. Sniffing time for both female and male urine was scored by a trained observer for a period of 3 min. Twenty-four hours later, mice that developed the anhedonia phenotype (<65% female urine preference; susceptible phenotype), as well as mice that did not develop the anhedonia phenotype (>75% female urine preference; resilient phenotype) were treated with either saline or (2*R*,6*R*)-HNK (10 mg kg^{-1}). Mice were re-tested for female urine preference 24 h later.

Pre-pulse inhibition. Mice were individually tested in acoustic startle boxes (SR-LAB, San Diego Instruments). After drug administration, mice were placed in the startle chamber for a 30-min habituation period. The experiment started

with a further 5-min adaptation period during which the mice were exposed to a constant background noise (67 dB), followed by five initial startle stimuli (120 dB, 40 ms duration each). Subsequently, animals were exposed to four different trial types: pulse alone trials (120 dB, 40 ms duration), three pre-pulse trials of 76 and 81 of white noise bursts (20 ms duration) preceding a 120 dB pulse by 100 ms, and background (67 dB) no-stimuli trials. Each of these trials was randomly presented five times. The dose of ketamine (30 mg kg^{-1}) was selected based on a dose–response experiment we performed in a previous study[36]. The percentage pre-pulse inhibition was calculated using the following formula: ((magnitude on pulse-alone trial − magnitude on pre-pulse + pulse trial)/magnitude on pulse-alone trial) × 100.

Drug discrimination. Mice were food-restricted until they reached 85% of their initial body weight and were maintained at 85% throughout the duration of the experiment. Animals were trained to lever press for food (20 mg sucrose pellets; TestDiet) in standard two-lever operant conditioning chambers (Coulbourn Instruments), under a fixed-ratio 5 schedule of reinforcement (FR5) in daily 30-min sessions. After stable responding was maintained over three consecutive sessions, mice were trained to discriminate ketamine (10 mg kg^{-1}) from saline under a double alternation schedule (that is, ketamine, ketamine, saline, saline), which required on average 40 training sessions. Mice received either ketamine (10 mg kg^{-1}; i.p.) or saline 15 min before the start of the 30-min session. Responding to the correct lever resulted in the delivery of a reward, while incorrect responding reset the FR for correct lever-responding. Drug discrimination test sessions were conducted when mice reached the following criteria: (1) first FR5 completed on the correct lever, and (2) ≥85% correct lever responding over the entire session. Fifteen minutes prior to the 30-min test sessions mice received either saline, ketamine (10 mg kg^{-1}), PCP (3 mg kg^{-1}) or (2*R*,6*R*)-HNK (10 and 50 mg kg^{-1}). At this stage, completion of the FR5 schedule on either lever resulted in the delivery of food reward. Lever response and pellet delivery were monitored and controlled by an automated computer system (Graphic State v3.1; Coulbourn Instruments).

Intravenous drug self-administration. *Apparatus.* Each operant chamber was equipped with one lever, a dipper liquid delivery system, a 22-gauge liquid swivel and a syringe pump (located outside the chamber). The lever was a balanced rocker arm that broke an infrared photo beam when 0.5 g of force was applied. Two stimulus lights were used; one was positioned to illuminate the translucent lever and the other was positioned above the liquid delivery recess. The lever light was illuminated during periods of water or drug availability; the second light was illuminated during water or drug delivery. The system was controlled by an integrated Coulbourn environmental control system and Med Associates interface.

Water training. Mice were first trained to complete an operant response for water reinforcement. Completion of the response requirements on the lever illuminated stimulus lights above a spout and delivered a small amount of water. Initially, the response requirement was one lever press (FR1); after completion of each 50 reinforcements the fixed ratio requirement was increased by one (FRX + 1). Mice were trained for 24 h per day for 4 days with free access to food.

Surgery. After completion of the water training, mice were surgically prepared with a catheter implanted in the jugular vein. Surgical procedures were performed under ketamine- (90 mg kg^{-1}, i.p.) and xylazine- (16 mg kg^{-1}, i.p.) induced anaesthesia. Silastic tubing (0.012 inch (0.30 mm) inner diameter) was implanted in the right jugular vein to the level of the atrium, passed subcutaneously and exited in the midscapular region. The catheter was connected to a tether/swivel system that was mounted to the skull of the mouse with dental cement.

Intravenous drug self-administration. Seven days after surgery, mice were placed in the operant chamber and given access (FR4) to 0.32, 1.0, 3.2 or 0 (saline) mg kg^{-1} drug per infusion for 5 days at each dose. Completion of each FR resulted in the illumination of the overhead house light and the stimulus light above the spout. Infusions of 5-8 μl (based on body weight) were given over a period of 15 s. A 30-s time-out period, during which house and stimulus lights were out, followed the completion of each infusion. Each mouse had access to drug for 6 h per day and free access to food and water 24 h per day. A 12-h light/dark cycle was maintained (lights on/off at 07:00/19:00). Each animal remained in its operant chamber for the duration of the experiment. A stimulus light illuminating the lever signalled drug availability. Only those animals with patent catheters at the end of the experiment were included in the analysis. The average number of reinforcements and drug intake during the last 3 days at each dose were used as dependent measures.

Rotarod. The rotarod test was conducted to compare the effects of ketamine, (2*S*,6*S*)-HNK and (2*R*,6*R*)-HNK on motor coordination. The experiment consisted of two phases: training phase (4 days) and a test phase (1 day). On each of the training days five trials (trial time: 3 min) were conducted with an inter-trial interval of two min. Mice were individually placed on the rotarod apparatus (IITC Life Science) and the rotor (3.75 inch diameter) accelerated from 5 to 20 r.p.m. over a period of three minutes. Latency to fall was recorded for each trial. Animals with an average of <100 s of latency to fall during the last training day were excluded from the experiment. On the test day (day 5), mice received (i.p.) injections of saline, (*R*,*S*)-KET (10 mg kg^{-1}), (2*S*,6*S*)-HNK (25 or 125 mg kg^{-1}) or (2*R*,6*R*)-HNK (25 or 125 mg kg^{-1}) and were tested in the rotating rod 5, 10, 15, 20, 30 and 60 min after injection using the same procedure described for the training days.

Tissue distribution and clearance measurements of ketamine and metabolites. At 10, 30, 60, or 240 min after drug administration mice were exposed to 3% isoflurane and subsequently decapitated. Trunk blood was collected in EDTA-containing tubes and centrifuged at 5,938*g* for 6 min (4 °C). Plasma was collected and stored at −80 °C until analysis. Whole brains were simultaneously collected, rinsed with PBS, immediately frozen in dry ice and stored at −80 °C until analysis.

The concentrations of (*R*,*S*)-ketamine and 6,6-dideuteroketamine and their respective metabolites in plasma and brain tissue were determined by achiral liquid chromatography-tandem mass spectrometry following a previously described method[33], with slight modifications. The analysis was accomplished using an Eclipse XDB-C18 guard column (4.6 × 12.5 mm) and a Varian Pursuit XRs 5 C18 analytical column (250 × 4.0 mm ID, 5 μm; Varian). The mobile phase consisted of ammonium acetate (5 mM, pH 7.6) as component A and acetonitrile as component B. A linear gradient was run as follows: 0 min 20% B; 5 min 20% B; 15 min 80% B; 20 min 20% B at a flow rate of 0.4 ml min^{-1}. The total run time was 30 min per sample. For plasma and brain samples, the calibration standards ranged from 10,000 ng ml^{-1} to 19.5 ng ml^{-1} for (*R*,*S*)-ketamine, (*R*,*S*)-norketamine, (2*R*,6*R*;2*S*,6*S*)-HNK, (*R*,*S*)-dehydronorketamine, (*R*,*S*)-d_2-ketamine, (*R*,*S*)-d_2-norketamine and d-(2*S*,6*S*;2*R*,6*R*)-HNK. The quantification of (*R*,*S*)-ketamine, (*R*,*S*)-d_2-ketamine and their respective metabolites was accomplished by calculating area ratios using d_4-ketamine (10 μl of 10 μg ml^{-1} solution) as the internal standard. The MS/MS analysis was performed using a triple quadrupole mass spectrometer model API 4000 system from Applied Biosystems/MDS Sciex equipped with Turbo Ion Spray (TIS) (Applied Biosystems). The data was acquired and analysed using Analyst version 1.4.2 (Applied Biosystems). Positive electrospray ionization data were acquired using multiple reaction monitoring (MRM) using the following transitions for (*R*,*S*)-ketamine studies: 238 → 125 (ketamine); 224 → 125 (norketamine); 222 → 177 (dehydronorketamine); 240 → 125 (HNK); 254 → 151 (HK) and (*R*,*S*)-d_2-ketamine studies: 240 → 125 (d_2-ketamine); 226 → 125 (d_2-norketamine); 223 → 178 (d-dehydronorketamine); 241 → 125 (d-(2,6)-HNK); 242-125 (d_2-(2,5)-HNK);(d_2-(2,4)-HNK) and 255 → 151 (d-(2,6)-HK).

MK-801 displacement binding. NMDAR binding assays were performed according to ref. 37, with minor modifications. Rat brains were homogenized and membrane fractions were collected. Aliquoted membranes were stored at −80 °C until use. Membrane pellets were washed five times with an ice-cold buffer (20 mM HEPES, 1 mM EDTA, pH 7.0) before use. The binding assays were set up in 96-well plates using 5 nM [^{3}H]MK-801 and rat brain membranes (100 μg per well) in a final volume of 125 μl per well in the NMDAR binding buffer (20 mM HEPES, 1 mM EDTA, 100 μM glutamate, 100 μM glycine, pH 7.0). Test compounds were first distributed in 96-well plates (25 μl per well at 5× final concentrations ranging from 0.1 nM to 10 μM, 11 points) in triplicate. The radioligand, [^{3}H]MK-801, was added (50 μl per well at 2.5× of final concentration of 5 nM) to all wells. Reactions started with the addition of 50 μl rat brain membrane and were incubated for 1 h in the dark at room temperature. The reactions were harvested via rapid filtration onto Whatman GF/B glass fibre filters pre-soaked with 0.3% polyethyleneimine using a 96-well Brandel harvester, followed by three quick washes each with 500 μl chilled wash buffer (50 mM Tris HCl, pH 7.4). Filters were microwave-dried and scintillation cocktail was then melted onto the filter mates on a hot plate. The radioactivity retained on the filters was counted in a MicroBeta scintillation counter. All assays were performed in triplicates.

Western blots. To purify synaptoneurosomes, mouse prefrontal cortex and hippocampi were dissected and homogenized in Syn-PER Reagent (ThermoFisher Scientific; 87793) with 1× protease and phosphatase inhibitor cocktail (ThermoFisher Scientific; 78440). The homogenate was centrifuged for 10 min at 1,200*g* at 4 °C. The supernatant was centrifuged at 15,000*g* for 20 min at 4 °C. After centrifugation, the pellet (synaptosomal fraction) was re-suspended and sonicated in N-PER Neuronal Protein Extraction Reagent (ThermoFisher Scientific; 87792). Protein concentration was determined via the BCA protein assay kit (ThermoFisher Scientific; 23227). Equal amount of proteins (10–40 μg as optimal for each antibody) for each sample was loaded into NuPage 4–12% Bis-Tris gel for electrophoresis. Gel transfer was performed with the TransBlot Turbo Transfer System (Bio-Rad) Nitrocellulose membranes with transferred proteins were blocked with 5% milk in TBST (TBS plus 0.1% Tween-20) for 1 h and kept with primary antibodies overnight at 4 °C. The following primary antibodies were used: phospho-eEF2 (at Thr56; Cell Signaling Technology; 2331), total eEF2 (Cell Signaling Technology; 2332), phospho-mTOR (at Ser2448; Cell Signaling Technology; 2971), total mTOR

(Cell Signaling Technology; 2983), GluA1 (Cell Signaling Technology; 2983), GluA2 (Cell Signaling Technology; 13607), BDNF (Santa Cruz Biotechnology; sc-546), and GAPDH (Abcam; ab8245). The next day, blots were washed three times in TBST and incubated with horseradish peroxidase conjugated anti-mouse or anti-rabbit secondary antibody (1:5,000 to 1:10,000) for 1 h. After three final washes with TBST, bands were detected using enhanced chemiluminescence (ECL) with the Syngene Imaging System (G:Box ChemiXX9). After imaging, the blots were incubated in the stripping buffer (ThermoFisher Scientific; 46430) for 10–15 min at room temperature followed by three washes with TBST. The stripped blots were incubated in blocking solution for 1 h and incubated with the primary antibody directed against total levels of the respective protein or GAPDH for loading control. Densitometric analysis of phospho- and total immunoreactive bands for each protein was conducted using Syngene's GenTools software. The values for the phosphorylated forms of proteins were normalized to phosphorylation-independent levels of the same protein. Phosphorylation-independent levels of proteins were normalized to GAPDH. Fold change was calculated by normalization to saline-treated control group for each protein or phosphoprotein.

qEEG. *Surgery.* qEEG experiments were performed according to ref. 38, with minor modifications. Mice were anaesthetized with isoflurane (3.5%) and maintained under anaesthesia (2–2.5%) throughout the surgery. Mice received analgesia (carprofen, 5 mg kg^{-1}, i.p.) before the start of surgery. An F20-EET radio-telemetric transmitter (Data Sciences International) was placed subcutaneously and its leads implanted over the dura above the frontal cortex (1.7 mm anterior to bregma) and the cerebellum (6.4 mm posterior to bregma). Animals recovered from surgery for 7 days before recordings.

qEEG recordings. For comparisons between saline, ketamine, and (2*R*,6*R*)-HNK, mice were singly housed and acclimated to the behavioural room for 24 h before qEEG recordings. qEEGs were recorded using the Dataquest A.R.T. acquisition system (Data Sciences International) with frontal qEEG recordings referenced to the cerebellum. Baseline qEEG (30 min) recordings were followed by an i.p. injection of saline, ketamine (10 mg kg^{-1}) or (2*R*,6*R*)-HNK (10 mg kg^{-1}) and a further 60 min of post-injection recordings. To assess effects of NBQX on (2*R*,6*R*)-HNK-induced changes in qEEG oscillations, mice were acclimated to the behavioural room 1.5–2 h before recordings. Baseline (30 min) recordings were followed by an i.p. injection of either saline or NBQX (10 mg kg^{-1}) and 30 min later mice received an injection (i.p.) of (2*R*,6*R*)-HNK (10 mg kg^{-1}) and recordings continued for 60 min after injection.

In vivo data analysis. qEEGs were analysed using custom-written MATLAB scripts (Version 2012a, Mathworks) and the mtspecgramc routine in the Chronux Toolbox (http://chronux.org[39]). Oscillation power in each bandwidth (delta = 1–3 Hz; theta = 4–7 Hz; alpha = 8–12 Hz; beta = 13–29 Hz; gamma = 30–80 Hz) was computed in 10-min bins from spectrograms for each animal.

Field recordings. Removal of the rat brains, as well as dissection of the hippocampi were performed in ice-cold ACSF bubbled with 95% O_2, 5% CO_2. The ACSF contained (in mM): 124 NaCl, 3 KCl, 1.25 NaH_2PO_4, 1.5 $MgCl_2$, 2.5 $CaCl_2$, 26 $NaHCO_3$ and 10 glucose. Hippocampal slices were cut at 400 μm using a vibratome and kept in a holding chamber at the interface of ACSF and humidified 95% O_2, 5% CO_2 for at least 1 h. For the fEPSPs, slices were transferred to a submersion-type recording chamber and perfused with ACSF (1–2 ml min^{-1}; room temperature). Picrotoxin (0.1 mM), CGP52432 (2 μM) and APV (80 μM) were added to block $GABA_A$, $GABA_B$ and NMDA receptors respectively. Concentric bipolar tungsten electrodes were placed in stratum radiatum to stimulate the Schaffer collateral afferents. Extracellular recording pipettes were filled with ACSF (3–5 MΩ) and placed in stratum radiatum of area CA1. Field potentials were evoked by monophasic stimulation (100 μs duration) at 0.1 Hz. The stimulus intensity was set at 150% of threshold intensity, resulting in fEPSPs amplitude of 0.1–0.3 mV. A stable baseline was recorded for at least 10 min. Vehicle and (2*R*,6*R*)-HNK were applied by perfusion over a period of 1 h followed by washout using ACSF. For AMPAR-mediated responses, peak fEPSP amplitudes and slopes, measured over a window of 1–4 ms following the rising phase of the response, are reported as percentage change from baseline. DNQX (50 μM) was bath-applied to ensure AMPA-mediated responses. Experiments were performed and analysed blind to treatment groups, using pCLAMP software (Molecular Devices).

Whole-cell patch-clamp recordings. Rats were euthanized by CO_2 asphyxiation followed by decapitation. Removal of the brains, as well as dissection and slicing of the hippocampi were performed in an ice-cold solution consisting of a mixture of equal parts of regular ACSF and sucrose-containing ACSF. ACSF was composed of (in mM): 125 NaCl, 26 $NaHCO_3$, 2.5 KCl, 1.25 NaH_2PO_4, 2 $CaCl_2$, 1 $MgCl_2$, and 25 glucose. Sucrose-containing ACSF was composed of (in mM): 230 sucrose, 2.5 KCl, 1.25 NaH_2PO_4, 26 $NaHCO_3$, 0.5 $CaCl_2$, 10 $MgSO_4$, and 10 glucose. Hippocampal slices of 300-μm thickness were cut using a vibratome (Leica VT1000S; Leica Microsystems Inc.) and transferred to an immersion chamber containing regular ACSF that was continuously bubbled with 95% O_2, 5% CO_2 and maintained in a water bath at 30 °C.

At the time of recordings, hippocampal slices were transferred to a 1-ml recording chamber, where they were superfused at 2 ml min^{-1} with ACSF that was continuously bubbled with 95% O_2, 5% CO_2. In all experiments, ACSF used to superfuse the slices contained the muscarinic antagonist atropine (0.5 μM) and the $GABA_A$ receptor antagonist picrotoxin (50 μM). Whole-cell patch-clamp recordings were obtained from the soma of CA1 stratum radiatum interneurons in hippocampal slices according to standard patch-clamp techniques using an EPC9 amplifier (HEKA Elektronik). The signals were filtered at 3 kHz and analysed using pCLAMP 10.3 or WinEDR v3.2.6 (University of Strathclyde, UK). The patch-clamp pipettes were pulled from a borosilicate glass capillary (1.2-mm OD) and had resistances between 3 and 5 MΩ when filled with internal solution. The internal pipette solution contained (in mM): 10 ethylene-glycol-bis(β-amino-ethylether)-*N*-*N*′-tetraacetic acid, 10 4-(2-hydroxyethyl)-1-piperazineethanesulfonic acid, 130 Cs-methane sulfonate, 10 CsCl, 2 $MgCl_2$, 5 lidocaine *N*-ethyl bromide, and 0.5% biocytin (pH adjusted to 7.3 with 340 mOsm CsOH). A specially adapted U-tube developed in the Albuquerque laboratory was used to apply NMDA (50 μM) to the neurons for the NMDA-evoked current experiments. NMDA-evoked currents and spontaneous AMPA-mediated excitatory postsynaptic currents (sEPSCs) were recorded at −40 mV and −60 mV respectively. A single neuron was studied in each slice. All experiments were carried out at room temperature (20–22 °C). The peak amplitude of NMDA-evoked currents was analysed using the pCLAMP v10.3 software, with baseline determined as the mean value obtained before drug application and the final (16 min) washout time point. Frequency and peak amplitude of AMPA sEPSCs were analysed using WinEDR v3.2.6.

Statistical analyses. Required sample sizes were estimated based on our past experience performing similar experiments. Experimentation and analysis were performed in a manner blinded to treatment assignments in all experiments with the exception of the whole-cell patch-clamp recordings and intravenous drug self-administration. For all blinded experiments, mice were randomly assigned to treatment groups. Statistical analyses were performed using GraphPad Prism software v6. By pre-established criteria, values greater than ±2 s.d. from individual group means were excluded from the analyses. All statistical tests were two-tailed, and significance was assigned at $P < 0.05$. Normality and equal variances between group samples were assessed using the Kolmogorov–Smirnov and Brown–Forsythe tests respectively. When normality and equal variance between sample groups was achieved, ANOVAs were followed by a Holm–Šídák post-hoc comparison when significance was reached, and significant results are indicated with asterisks in the figures. As a secondary analysis, pairwise comparisons at each equivalent dose were performed followed by multiple comparison corrections, where appropriate, and are reported in Supplementary Information Table 1. Where normality or equal variance of samples failed, non-parametric one-way ANOVAs (Kruskal–Wallis one-way ANOVA on ranks or Friedman repeated-measures one-way ANOVA on ranks) were performed, followed by Dunn's correction. For assessment of the NSF test results, Kaplan–Meier survival analysis was used followed by the Mantel–Cox log-rank test. The sample sizes (biological replicates), specific statistical tests used, and the main effects of our statistical analyses for each experiment are reported in Supplementary Information Table 1.

34. Donahue, R. J., Muschamp, J. W., Russo, S. J., Nestler, E. J. & Carlezon, W. A. Jr. Effects of striatal ΔFosB overexpression and ketamine on social defeat stress-induced anhedonia in mice. *Biol. Psychiatry* **76,** 550–558 (2014).
35. Malkesman, O. *et al.* The female urine sniffing test: a novel approach for assessing reward-seeking behavior in rodents. *Biol. Psychiatry* **67,** 864–871 (2010).
36. Zanos, P. *et al.* The prodrug 4-chlorokynurenine causes ketamine-like antidepressant effects, but not side effects, by NMDA/glycineb-site inhibition. *J. Pharmacol. Exp. Ther.* **355,** 76–85 (2015).
37. Chiu, J. *et al.* Chronic ethanol exposure alters MK-801 binding sites in the cerebral cortex of the near-term fetal guinea pig. *Alcohol* **17,** 215–221 (1999).
38. Raver, S. M., Haughwout, S. P. & Keller, A. Adolescent cannabinoid exposure permanently suppresses cortical oscillations in adult mice. *Neuropsychopharmacology* **38,** 2338–2347 (2013).
39. Bokil, H., Andrews, P., Kulkarni, J. E., Mehta, S. & Mitra, P. P. Chronux: a platform for analyzing neural signals. *J. Neurosci. Methods* **192,** 146–151 (2010).

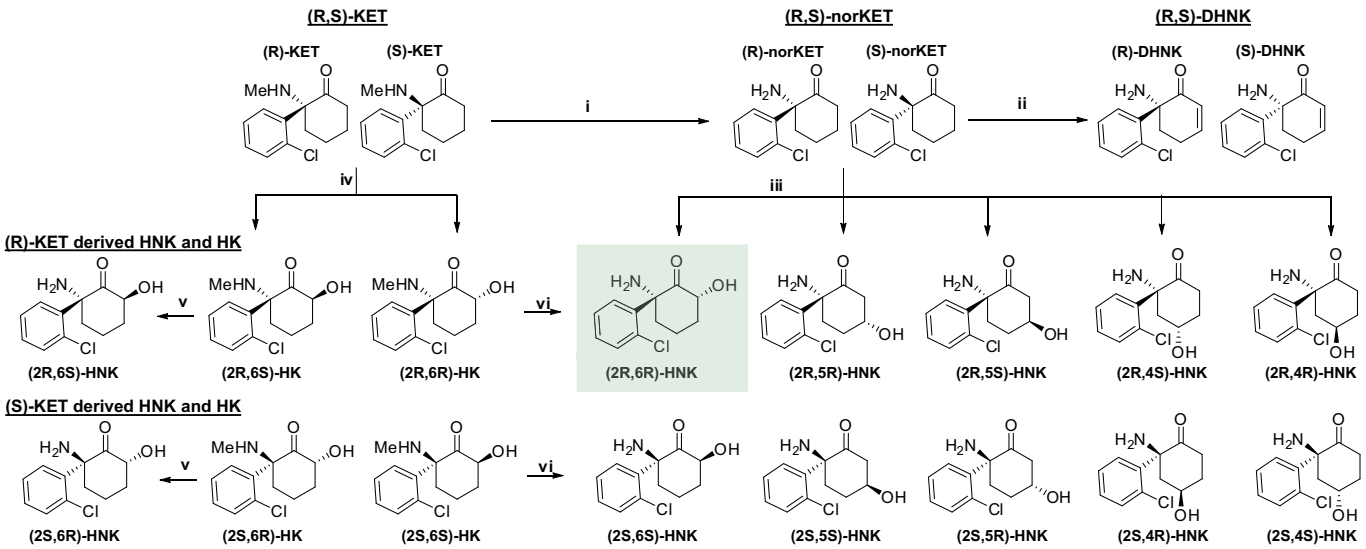

Extended Data Figure 1 | The metabolic transformations of ketamine *in vivo*. Ketamine is metabolised *in vivo* via P450 enzymatic transformations. **i**, (*R*,*S*)-KET is selectively demethylated to give (*R*,*S*)-norketamine (norKET). **ii**, NorKET can be then dehydrogenated to give (*R*,*S*)-dehydronorketamine (DHNK). **iii**, Alternatively, norKET can be hydroxylated to give the hydroxynorketamines (HNKs). **iv**, (*R*,*S*)-KET can also be hydroxylated at the 6 position to give either the *E*-6-hydroxyketamine ((2*S*,6*R*;2*R*,6*S*)-HK) or *Z*-6-hydroxyketamine ((2*S*,6*S*;2*R*,6*R*)-HK). **v**, Demethylation of (2*S*,6*R*;2*R*,6*S*)-HK yields the production of (2*S*,6*R*;2*R*,6*S*)-HNK. **vi**, Demethylation of (2*S*,6*S*;2*R*,6*R*)-HK further gives (2*S*,6*S*;2*R*,6*R*)-HNK.

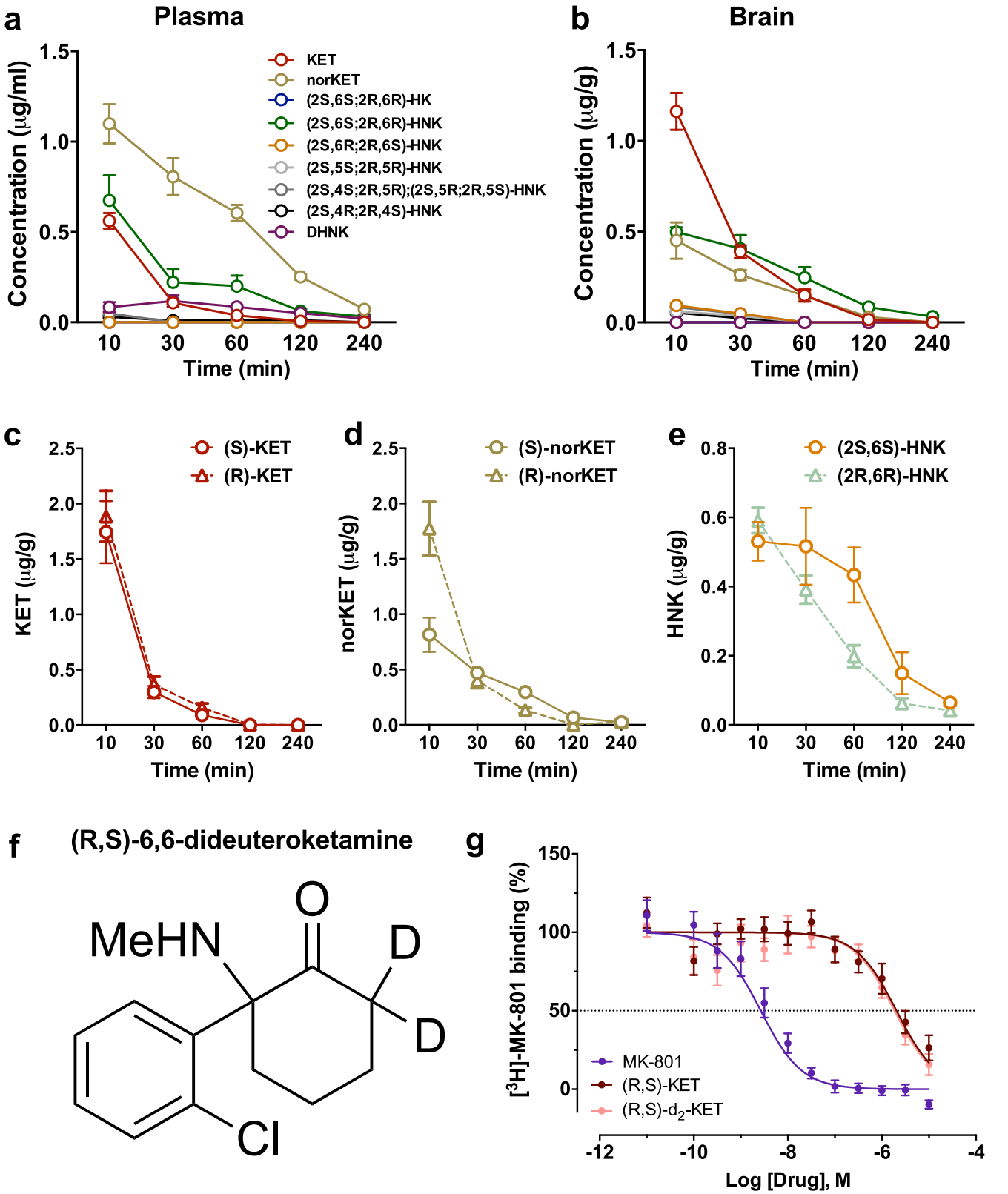

Extended Data Figure 2 | Circulating levels of ketamine and its metabolites following i.p. administration in mice. a, **b**, Plasma (**a**) and brain (**b**) levels of ketamine and its metabolites after administration of (*R*,*S*)-KET (10 mg kg^{-1}) in mice. **c**, **d**, Brain levels of KET (**c**), norKET (**d**) and HNK (**e**) following administration of (*S*)- and (*R*)-KET. **f**, **g**, Chemical structure of (*R*,*S*)-6,6-dideuteroketamine ((*R*,*S*)-d_2-KET) (**f**), which displaces [^{3}H]MK-801 binding with a similar affinity to (*R*,*S*)-KET ((*R*,*S*)-KET: K_i = 799 nM; (*R*,*S*)-d_2-KET: K_i = 883 nM) (**g**). See Supplementary Table 1 for statistical analyses and *n* numbers.

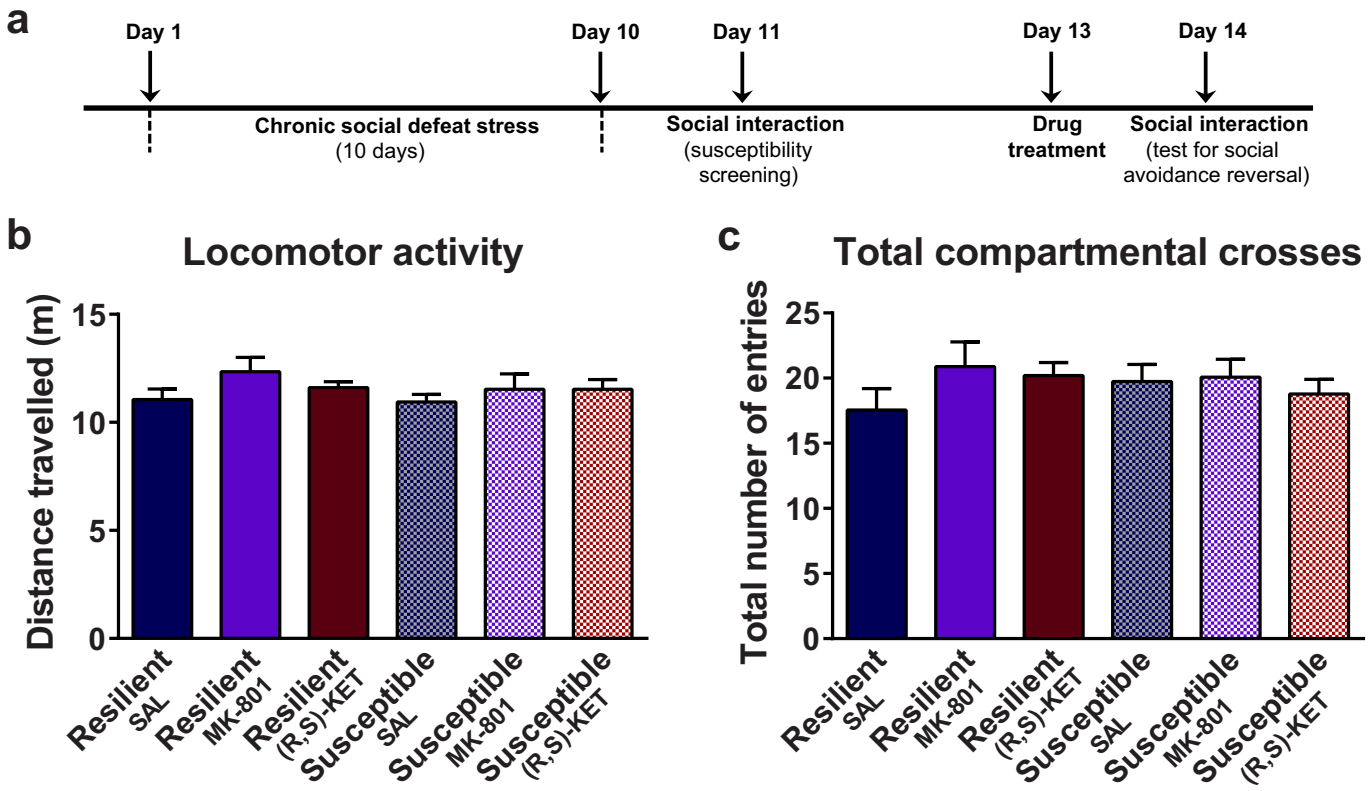

Extended Data Figure 3 | Additional social defeat stress data. a, Chronic social defeat stress and social interaction/avoidance test timeline. **b**, **c**, 24 h after administration, neither (*R*,*S*)-KET nor MK-801 affected locomotor activity (**b**) or total number of compartmental crosses in the social interaction apparatus (**c**). Data are mean ± s.e.m. ***$P < 0.001$. See Supplementary Table 1 for statistical analyses and *n* numbers.

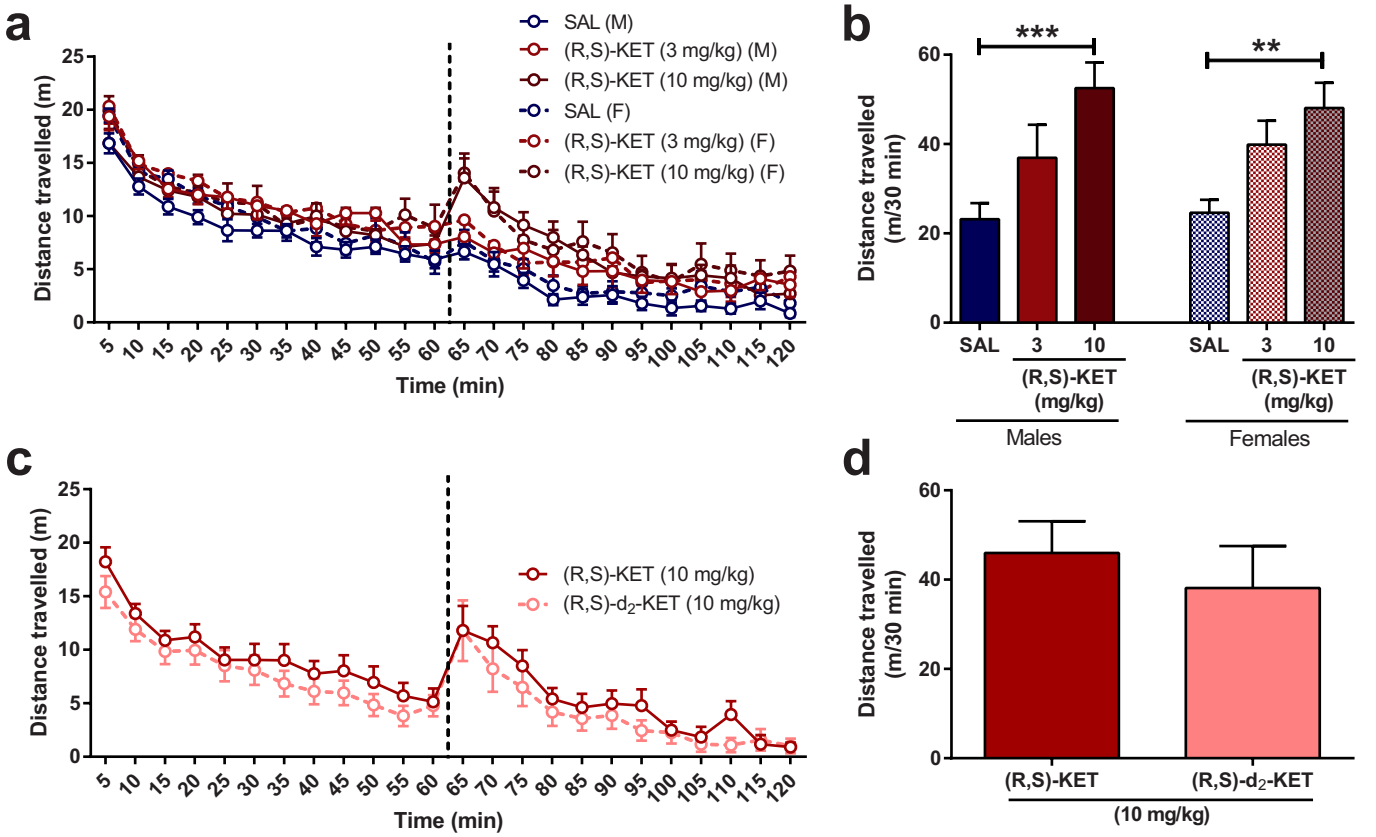

Extended Data Figure 4 | Locomotor effects of (*R*,*S*)-KET and (*R*,*S*)-d_2-KET. After recording baseline activity for 60 min, mice received drug (marked by a vertical dashed line) and locomotor activity was monitored for another 1 h. **a**, **b**, Administration of (*R*,*S*)-KET (10 mg kg^{-1}), induced hyperlocomotor responses equally in both male and female mice. **c**, **d**, (*R*,*S*)-KET and (*R*,*S*)-d_2-KET were equally potent in inducing a hyperlocomotor response at the dose of 10 mg kg^{-1}. Data are mean ± s.e.m. $^*P < 0.05$, $^{**}P < 0.01$ (see Supplementary Table 1 for statistical analyses and *n* numbers).

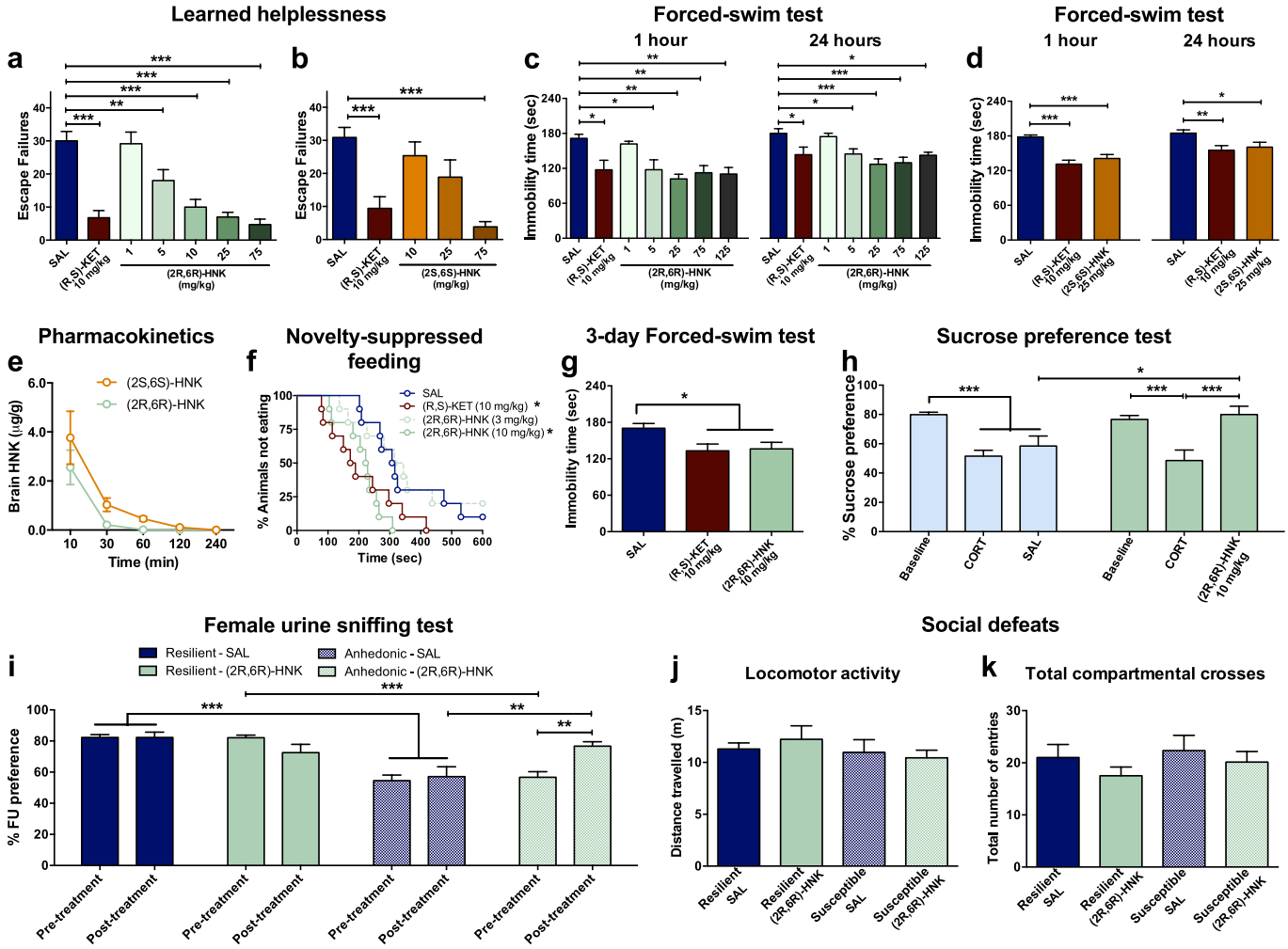

Extended Data Figure 5 | Acute and sustained antidepressant and anti-anhedonic effects of (2*R*,6*R*)- and (2*S*,6*S*)-HNK. a, A single injection of (2*R*,6*R*)-HNK resulted in dose-dependent antidepressant-like responses in the learned helplessness test at the doses of 5–75 mg kg^{-1}. **b**, A single injection of (2*S*,6*S*)- HNK induced antidepressant-like effects in the learned helplessness test at the dose of 75 mg kg^{-1}. **c**, Administration of (2*R*,6*R*)-HNK induced dose-dependent antidepressant effects in the 1- and 24-h FST. **d**, Administration of (2*S*,6*S*)-HNK at the dose of 25 mg kg^{-1} induced antidepressant effects in the 1- and 24-h FST. **e**, Despite the greater antidepressant efficacy of (2*R*,6*R*)-HNK, administration of (2*S*,6*S*)-HNK (HNK) results in higher brain hydroxynorketamine levels compared to (2*R*,6*R*)-HNK. **f**, (2*R*,6*R*)-HNK manifested dose-dependent antidepressant-like effects in the NSF test. **g**, Similar to (*R*,*S*)-KET, the antidepressant-like effects of (2*R*,6*R*)-HNK in the FST persisted for at least 3 days after treatment. **h**, A single administration of (2*R*,6*R*)-HNK reversed chronic corticosterone-induced decreases in sucrose preference. **i**, A single administration of (2*R*,6*R*)-HNK reversed chronic corticosterone-induced decrease in female urine sniffing preference, specifically in mice that developed an anhedonic phenotype. Administration of (2*R*,6*R*)-HNK was not associated with changes in locomotor activity (**j**) or total compartmental crosses in the social interaction test after chronic social defeat stress (**k**). Data are mean ± s.e.m. $^{*}P < 0.05$, $^{**}P < 0.01$, $^{***}P < 0.001$ (see Supplementary Table 1 for statistical analyses and *n* numbers).

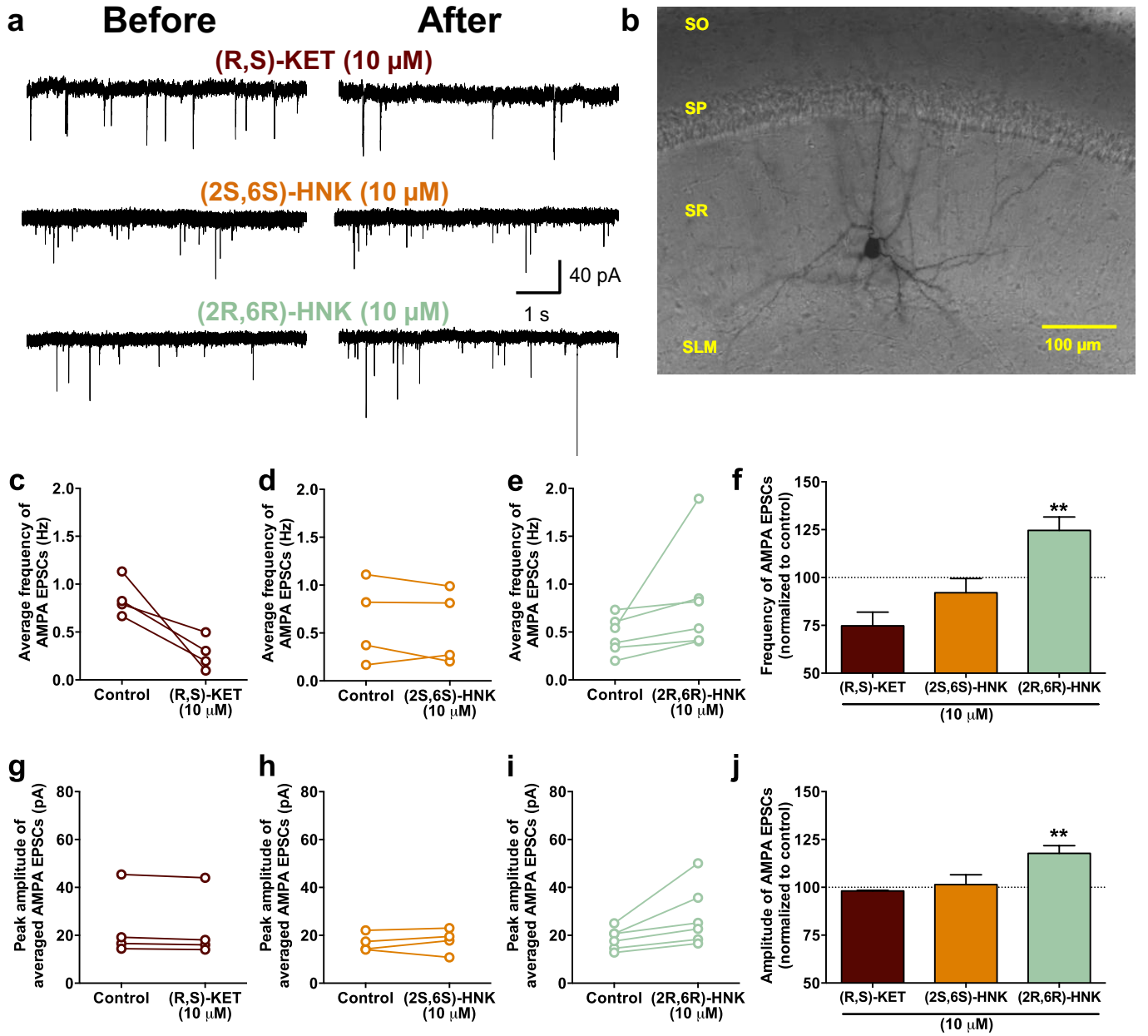

Extended Data Figure 6 | (2*R*,6*R*)-HNK rapidly increases the frequency and amplitude of AMPAR spontaneous excitatory postsynaptic currents in the hippocampus. a, Representative traces of spontaneous excitatory postsynaptic currents (sEPSCs) mediated via AMPARs during baseline (before) and 20 min after drug administration. **b**, Example CA1 stratum radiatum interneuron recorded from a rat hippocampal slice. **c**–**j**, Twenty-minute exposure of (2*R*,6*R*)-HNK (**e**, **i**), but not (*R*,*S*)-(KET) (**c**, **g**) or (2*S*,6*S*)-HNK (**d**, **h**), increased AMPA sEPSCs frequency and amplitude compared to baseline. Data are mean ± s.e.m. $*P < 0.05$, $**P < 0.01$, $***P < 0.001$ (see Supplementary Table 1 for statistical analyses and *n* numbers). SLM, stratum lacunosum-moleculare; SO, stratum oriens; SP, stratum pyramidale; SR, stratum radiatum.

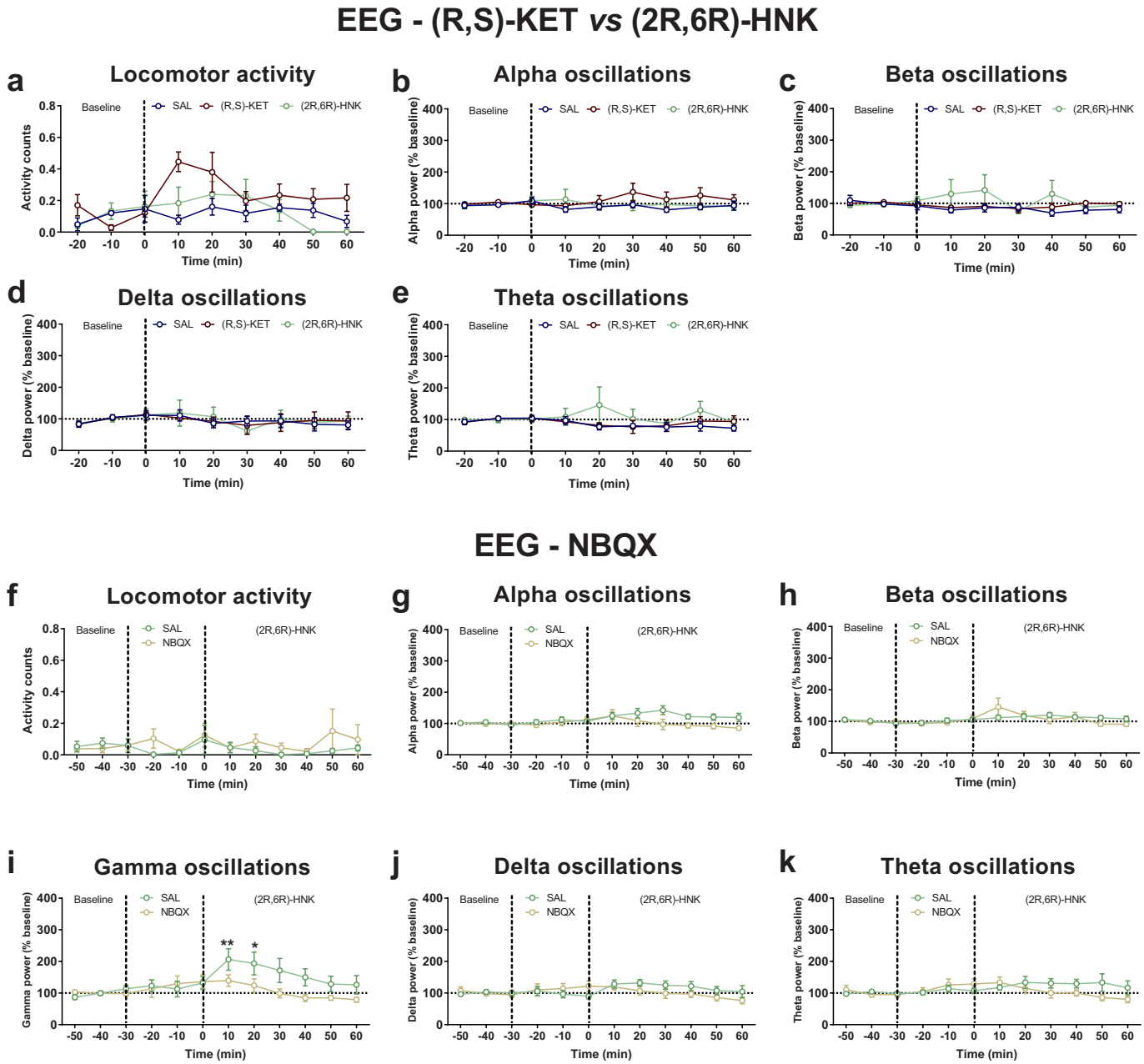

Extended Data Figure 7 | Administration of the AMPAR antagonist, NBQX, prevents (2*R*,6*R*)-HNK-induced increases in gamma oscillations *in vivo*. **a**, Administration of (*R*,*S*)-KET, but not (2*R*,6*R*)-HNK, increased locomotor home-cage activity of mice. **b**–**e**, Neither (*R*,*S*)-KET nor (2*R*,6*R*)-HNK altered cortical alpha (**b**), beta (**c**), delta (**d**) or theta (**e**) oscillations *in vivo*. **f**–**k**, Pre-treatment with the AMPAR antagonist, NBQX, did not change the locomotor activity (**f**), alpha (**g**), beta (**h**), delta (**j**) or theta (**k**) oscillations, but it prevented (2*R*,6*R*)-HNK-induced increases of gamma oscillations *in vivo* (**i**). Data are mean ± s.e.m. $*P < 0.05$, $**P < 0.01$ (see Supplementary Table 1 for statistical analyses and *n* numbers).

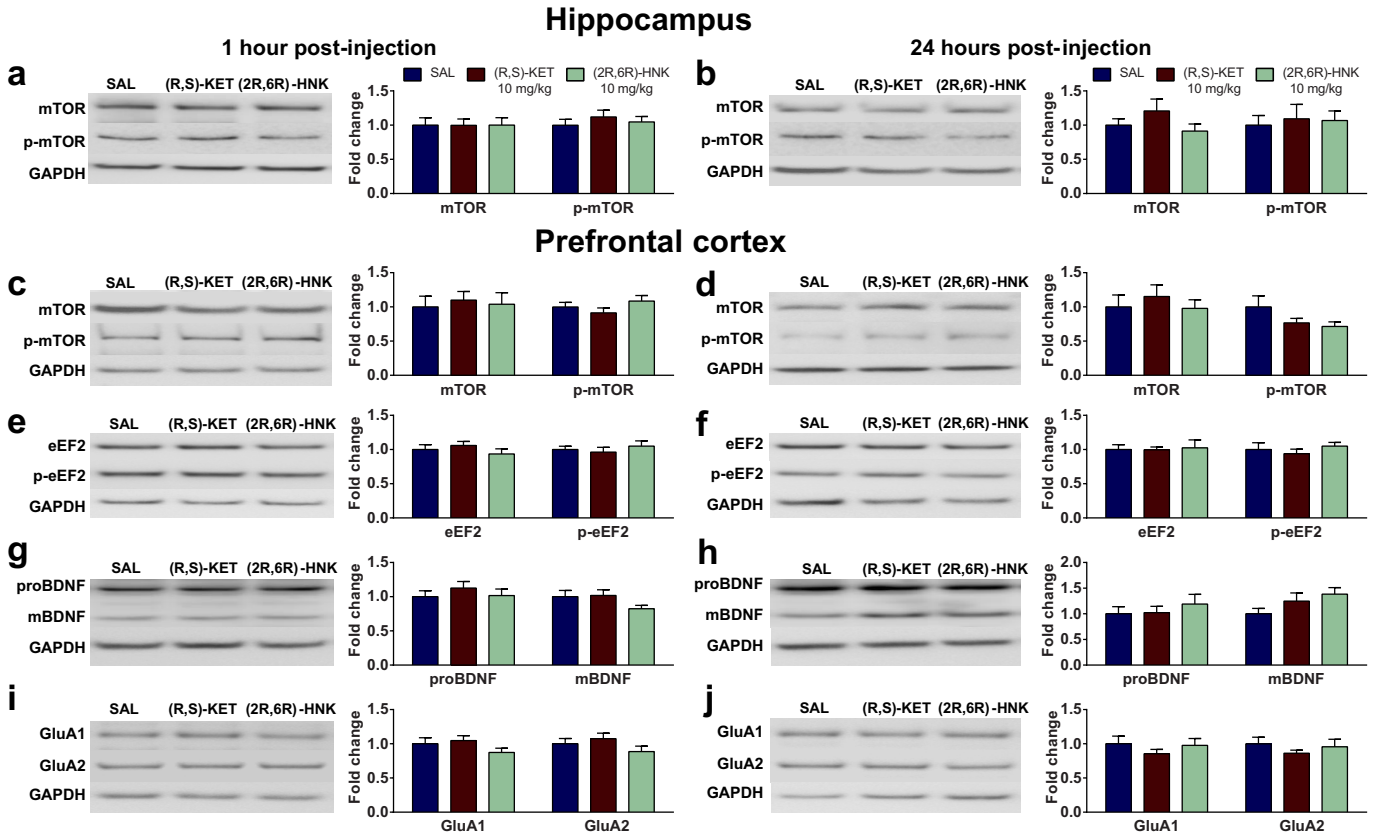

Extended Data Figure 8 | Effects of (2*R*,6*R*)-hydroxynorketamine on protein and protein phosphorylation levels in synaptoneurosomes. **a**, **b**, A single administration of (*R*,*S*)-KET (10 mg kg^{-1}) or (2*R*,6*R*)-HNK (10 mg kg^{-1}), did not alter levels of mTOR or phosphorylated mTOR in the hippocampus 1 h (**a**) or 24 h (**b**) after injection. **c**–**j**, Administration of (*R*,*S*)-KET or (2*R*,6*R*)-HNK did not alter levels of mTOR/phosphorylated mTOR (**c**, **d**), eEF2/phosphorylated eEF2 (**e**, **f**), proBDNF/mBDNF (**g**, **h**), or GluA1/GluA2 (**i**, **j**), in the prefrontal cortex of mice. The values for the phosphorylated forms of proteins were normalized to phosphorylation-independent levels of the same protein. Phosphorylation-independent levels of proteins were normalized to GAPDH. Data are mean ± s.e.m, and were normalized to the saline-treated control group for each protein. Images are cropped; see Supplementary Fig. 1 for complete blot images. *$P < 0.05$ (see Supplementary Table 1 for statistical analyses and *n* numbers).

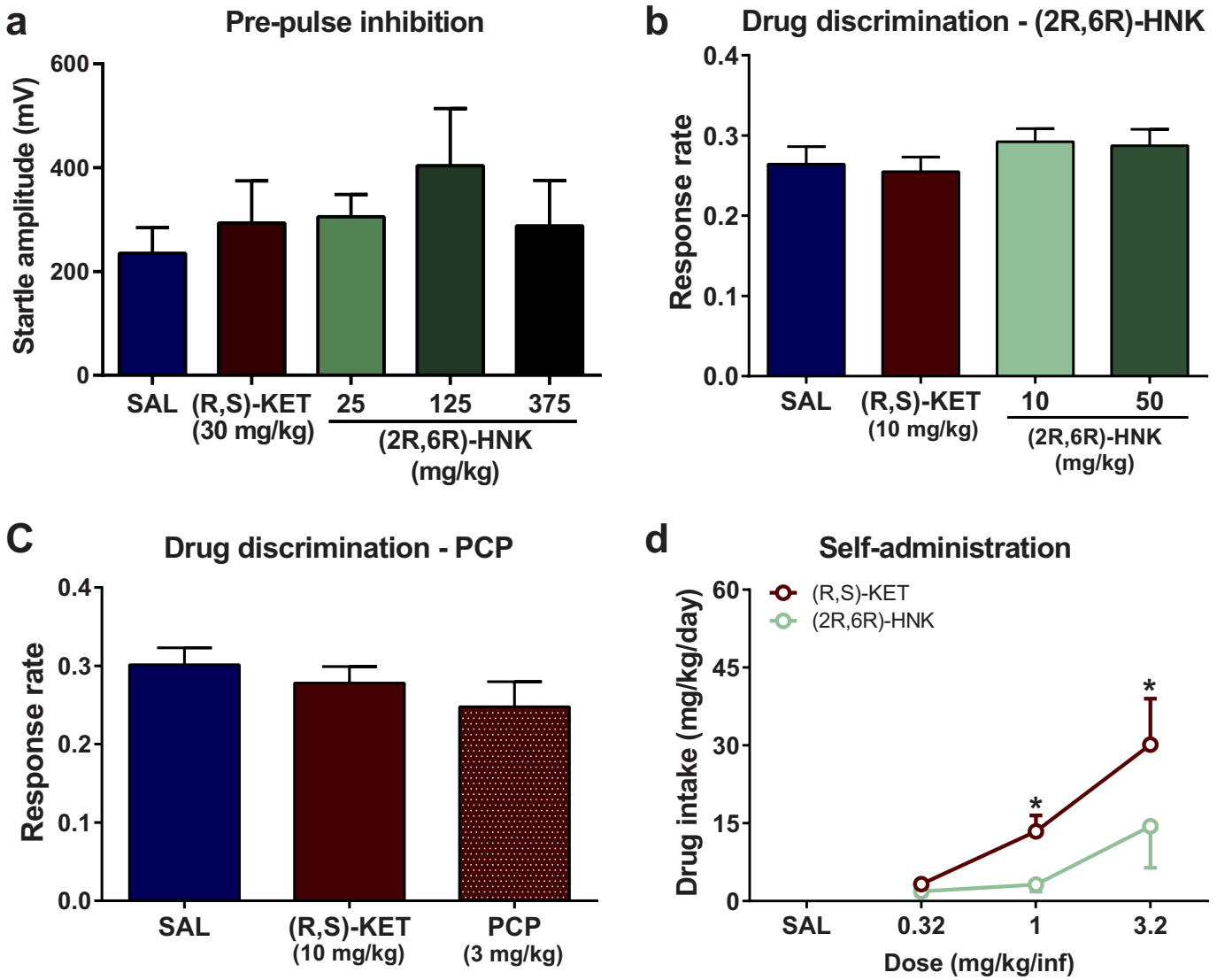

Extended Data Figure 9 | (2*R*,6*R*)-HNK administration does not alter startle amplitude, drug discrimination rate or self-administration drug intake. a, Startle amplitude as measured in the pre-pulse inhibition task was not affected by administration of (*R*,*S*)-KET or (2*R*,6*R*)-HNK. **b**, **c**, Response rate of overall lever pressing per sec in the drug discrimination model was not changed by administration of (*R*,*S*)-KET, (2*R*,6*R*)-HNK (**b**) or PCP (**c**). **d**, Unlike ketamine, (2*R*,6*R*)-HNK did not alter drug intake in the self-administration task in mice. Data are mean ± s.e.m. $*P < 0.05$ (see Supplementary Table 1 for statistical analyses and *n* numbers).